HAL
open science

Variability and trends in total and vertically resolved stratospheric ozone

D. Brunner, J. Staehelin, J. A. Maeder, I. Wohltmann, G. E. Bodeker

To cite this version:

D. Brunner, J. Staehelin, J. A. Maeder, I. Wohltmann, G. E. Bodeker. Variability and trends in total and vertically resolved stratospheric ozone. Atmospheric Chemistry and Physics Discussions, 2006, 6 (4), pp.6317-6368. hal-00301805

HAL Id: hal-00301805

https://hal.science/hal-00301805v1

Submitted on 18 Jun 2008

HAL is a multi-disciplinary open access archive for the deposit and dissemination of scientific research documents, whether they are published or not. The documents may come from teaching and research institutions in France or abroad, or from public or private research centers.

L'archive ouverte pluridisciplinaire **HAL**, est destinée au dépôt et à la diffusion de documents scientifiques de niveau recherche, publiés ou non, émanant des établissements d'enseignement et de recherche français ou étrangers, des laboratoires publics ou privés.

Atmos. Chem. Phys. Discuss., 6, 6317–6368, 2006
www.atmos-chem-phys-discuss.net/6/6317/2006/
© Author(s) 2006. This work is licensed
under a Creative Commons License.

Atmospheric Chemistry and Physics Discussions

Variability and trends in total and vertically resolved stratospheric ozone

D. Brunner[1,*], J. Staehelin[1], J. A. Maeder[1], I. Wohltmann[2], and G. E. Bodeker[3]

[1]Institute for Atmospheric and Climate Science, ETH Zurich, Switzerland
[2]Alfred Wegner Institute, Potsdam, Germany
[3]National Institute of Water and Atmospheric Research (NIWA), New Zealand
[*]now at: Empa – Materials Science and Technology, Dübendorf, Switzerland

Received: 22 June 2006 – Accepted: 29 June 2006 – Published: 12 July 2006

Correspondence to: D. Brunner (dominik.brunner@empa.ch)

Abstract

Trends in ozone columns and vertical distributions were calculated for the period 1979–2004 based on the three-dimensional ozone data set CATO (Candidoz Assimilated Three-dimensional Ozone) using a multiple linear regression model. CATO has been reconstructed from TOMS, GOME and SBUV total column ozone observations in an equivalent latitude and potential temperature framework and offers a pole to pole coverage of the stratosphere on 15 potential temperature levels. The regression model includes explanatory variables describing the influence of the quasi-biennial oscillation, volcanic eruptions, the solar cycle, the Brewer-Dobson circulation, Arctic ozone depletion, and the increase in stratospheric chlorine. The effects of displacements of the polar vortex and jet streams due to planetary waves, which may significantly affect trends at a given geographical latitude, are eliminated in the equivalent latitude framework. Ozone variability is largely explained by the QBO and stratospheric aerosol loading and the spatial structure of their influence is in good agreement with previous studies. The solar cycle signal peaks at about 30 to 35 km altitude which is lower than reported previously, and no negative signal is found in the tropical lower stratosphere. The Brewer-Dobson circulation shows a dominant contribution to interannual variability at both high and low latitudes and accounts for some of the ozone increase seen in the northern hemisphere since the mid-1990s. Arctic ozone depletion significantly affects the high northern latitudes between January and March and extends its influence to the mid-latitudes during later months. The vertical distribution of the ozone trend shows distinct negative trends at about 18 km in the lower stratosphere with largest declines over the poles, and above 35 km in the upper stratosphere. A narrow band of large negative trends extends into the tropical lower stratosphere. Assuming that the observed negative trend before 1995 continued to 2004 cannot explain the ozone changes since 1996. A model accounting for recent changes in EESC, aerosols and Eliassen-Palm flux, on the other hand, closely tracks ozone changes since 1995.

1 Introduction

Anthropogenic stratospheric ozone depletion has been discussed since the early 1970s (Crutzen, 1970; Johnston, 1971; Molina and Rowland, 1974; Stolarski and Cicerone, 1974). In 1985 the Antarctic ozone hole was detected (Farman et al., 1985) and in 1988 significant winter time decreases were first documented for northern midlatitudes from ground-based measurements and later confirmed by satellite observations (Stolarski et al., 1991). Polar and midlatitude trends were subsequently reported in many studies. For an overview see Staehelin et al. (2001); World Meteorological Organization (2003).

During the 1990s a number of studies provided evidence that part of the observed trends can be attributed to processes other than anthropogenic ozone depletion. Such processes included decadal scale climate variability related to the North Atlantic Oscillation (NAO) or Arctic Oscillation (AO) (e.g. Appenzeller et al., 2000), tropopause altitude (Steinbrecht et al., 1998), and changes in the strength of the Brewer-Dobson circulation (Fusco and Salby, 1999; Hadjinicolaou et al., 2002). These factors were found to affect the trends in addition to the solar cycle, the quasi-biennial oscillation (QBO) and volcanic eruptions which had been appreciated already in previous assessments of stratospheric ozone depletion (World Meteorological Organization, 1995).

As consequence of the Montreal Protocol and its amendments the emissions of anthropogenic ozone depleting substances (ODSs) decreased. According to the temporal evolution of ODSs in the stratosphere, chemical ozone depletion probably reached a maximum around the late 1990s and slowly decreased thereafter. Therefore, the discussion started whether the effect of the Montreal Protocol on the ozone layer can already be identified in the present observations (Weatherhead et al., 2000; Reinsel et al., 2002; Weatherhead and Andersen, 2006). Newchurch et al. (2003) reported on first signs of recovery analyzing upper stratospheric ozone trends while Reinsel et al. (2005) reported that the linear trend in total column ozone had changed significantly beyond 1996 poleward of 40°. Identifying ozone recovery requires both detection of a

positive change in ozone tendency as well as attribution of that change to decreasing ODSs. Questions remain whether all other factors influencing ozone such as solar cycle or planetary wave forcing were properly accounted for in these studies (Steinbrecht et al., 2004; Dhomse et al., 2006). An important problem in all trend studies using satellite data arises from the fact that the ozone time series available for fitting a statistical model are relatively short in comparison to the timescales of variability of some of the explanatory variables. This is additionally complicated by correlations among these variables which limits our ability to separate different effects (Solomon et al., 1996; Salby et al., 1997). Extending the time series out to 2004 now allows for a better separation between solar cycle, volcanic eruptions and QBO effects. Unlike the previous two solar cycles the latest one (no. 23) was not synchronized with a major volcanic eruption and the QBO was in opposite phase during solar maximum than previously.

In this study we present the results of a multiple linear regression analysis applied to the quasi-3-D ozone data set CATO (CANDIDOZ Assimilated Three-dimensional Ozone) (Brunner et al., 2006). In CATO the stratospheric ozone distribution is represented in an equivalent latitude – potential temperature coordinate system which has the advantage that it closely follows the contours of a passive tracer which are distorted by planetary waves (Schoeberl et al., 1989). Sharp gradients e.g. across the edge of the polar vortex are much better preserved in this coordinate system than in a standard zonal mean view (Bodeker et al., 2001). In addition, an important part of dynamical variability associated with planetary waves and meridional displacements of the vortex is efficiently removed in this framework. These effects not only account for a large fraction of the variability in total ozone observations but also contribute to long-term trends in a given geographical latitude band as demonstrated by Wohltmann et al. (2006)[1]. Since CATO was reconstructed from satellite total ozone measurements it provides a unique view of the vertical distribution of stratospheric ozone that is fully

[1]Wohltmann, I., Lehmann, R., Rex, M., Brunner, D., and Mäder, J. A.: A process-oriented regression model for column ozone, J. Geophys. Res., submitted, 2006.

consistent with the total columns. It extends from pole to pole and currently covers the period 1979 to 2004 without gaps.

So far only few satellite-based studies are available on long-term ozone trends in the lower stratosphere where the bulk of ozone resides. However, knowledge of the vertical distribution of the trends is essential as it provides additional insight into the processes governing stratospheric ozone. Most previous studies were restricted to altitudes higher than 20 km due to limitations in profile retrievals from SAGE (particularly SAGE I) and SBUV which were additionally complicated during periods of enhanced volcanic aerosol. Wang et al. (2002) presented an improved algorithm for SAGE II retrievals below 20 km which allowed calculating ozone trends down to the tropopause for the period 1984 to 1999. In an earlier study by Randel and Wu (1999) total column data from TOMS were combined with SAGE I/II profile data to calculate the residual amount between the tropopause and 20 km altitude. The present study complements these analyzes as it is based on a completely independent data set which is more complete in terms of temporal and spatial coverage.

Section 2.1 presents an overview of CATO which has been described in detail in Brunner et al. (2006). The statistical model is described in Sect. 2.2. Results of the regression analysis are then shown in Sect. 3 both for total ozone and the corresponding vertical distribution. We highlight the influence of the QBO, solar cycle, volcanic eruptions, planetary wave forcing, and polar ozone depletion, and analyze the trend attributable to the anthropogenic release of ODSs. Finally, in Sect. 3.3 we study the recent evolution of ozone and show that since 1996 there has been a statistically significant change in ozone trend. By using the regression model to attribute these recent changes to the explanatory variables included in the model, we show to what extent these changes result from changes in stratospheric ODSs concentrations and hence to what extent these changes can be interpreted as a sign of ozone recovery.

2 Data and methods

2.1 Reconstructed ozone data set CATO

CATO is a statistically reconstructed data set describing the vertical distribution of ozone in the stratosphere and the horizontal distribution of residual ozone columns in the troposphere. It currently covers the period January 1979 to December 2004. The tropospheric columns are represented in geographical longitude (λ) and latitude (ϕ) (with $10^\circ \times 6^\circ$ resolution) and the stratospheric distribution in equivalent latitude (ϕ_E) and potential temperature (θ) coordinates (6° horizontal resolution and 15 potential temperature levels between 326 K and 1445 K). The reconstruction is based on combining satellite total ozone observations with meteorological information on short-term meridional excursions of air masses due to isentropic transport using a data assimilation approach. The method is described in detail in Brunner et al. (2006) where it is also shown that CATO agrees reasonably well with observations from ozonesondes and HALOE including a realistic description of seasonal and interannual variability. Significant deviations from observed profiles were found however at high polar latitudes as well as in the tropical lower stratosphere.

An important advantage of CATO is that it has a pole to pole coverage and spans the complete period 1979 to 2004 including the months following the eruption of Mount Pinatubo. Moreover, CATO is based on the carefully homogenized NIWA assimilated total ozone data base where observations from the series of TOMS, GOME and SBUV instruments are combined into a single homogeneous data set by correcting for biases with respect to ground-based Dobson stations and for biases between satellite instruments observed during periods of overlap (Bodeker et al., 2001, 2005).

Because the reconstruction method is based on the assumption that ozone behaves like a passive tracer on time scales of these short-term meridional excursions, it fails to produce a realistic distribution above about 30 km altitude where the chemical lifetime becomes short. Therefore, CATO is relaxed towards the monthly mean climatology of Fortuin and Kelder (1998) on isentropes higher than 820 K with a relaxation timescale

decreasing from 70 days at 820 K to 2.5 days at 1445 K. As a consequence, any variability above 820 K is damped. We have therefore created a second data set where the relaxation above 820 K was replaced by the assimilation of vertical profiles from the SBUV and SBUV/2 version 8 data (see Brunner et al., 2006). This data set is only used for sensitivity checks and for the interpretation of variability and trends above 30 km altitude. Note that the two versions of CATO differ slightly in their vertical distribution whereas the total columns are basically identical because of the assimilation of total column observations.

CATO has been used by Wohltmann et al. (2005) to reconstruct an "integrated equivalent latitude proxy" for individual Dobson stations for use in regression analysis of long-term ozone trends. The station-specific proxy time series were obtained by vertically integrating the 1979–2004 mean CATO ozone field $\chi_{\mathrm{clim}}(\phi_E, \theta)$ along the equivalent latitude profiles $\phi_E(\lambda, \phi, \theta)$ calculated at each measurement point and time. Wohltmann et al. (2006)[1] demonstrated that this proxy is able to explain a large part of total ozone variability measured at these stations.

2.2 Regression model

The set of explanatory variables (or proxies) chosen for the regression model describes the influence of the solar cycle, the QBO, stratospheric aerosol loading following volcanic eruptions, the strength of the Brewer-Dobson circulation, and the anthropogenic impact on ozone through release of ozone depleting substances (ODSs). A linear response of ozone to changes in these variables is assumed though the response may be different for different months of the year. The proxies are selected to model as closely as possible the most relevant processes influencing stratospheric ozone variability. A more detailed motivation for the choice of explanatory variables we use here is given in the companion paper by Wohltmann et al. (2006)[1]. Note that in contrast to other trend studies the influence of various climate modes such as the North Atlantic Oscillation (NAO) or the El Niño – Southern Oscillation (ENSO) are not included explicitly. NAO and other climate modes may change the position of troughs and ridges of planetary

waves and hence modulate the altitude of the tropopause (Appenzeller et al., 2000; Weiss et al., 2001) and invoke meridional advection of ozone from regions of higher or lower climatological mean concentrations (Koch et al., 2002). While this may explain a significant fraction of ozone variability at a given point on the globe, much of these effects are eliminated when adopting an equivalent latitude and potential temperature framework (cf. Wohltmann et al., 2005) which is the approach followed here. In addition, NAO influences the propagation of waves into the stratosphere and hence the deposition of wave momentum driving the Brewer-Dobson circulation (Rind et al., 2005). This further affects the polar vortex which is stronger when the NAO is in a positive phase (Schnadt and Dameris, 2003). These effects are again accounted for, at least qualitatively, by including Eliassen-Palm (EP) flux as a proxy for the Brewer-Dobson circulation (Fusco and Salby, 1999) and the volume of polar stratospheric clouds (PSC) to describe Arctic ozone loss (Rex et al., 2004).

The setup of the regression model is similar to that by Stolarski et al. (1991) or Ziemke et al. (1997) and is formulated in one of the two following forms

$$Y(t) = a(t) + b(t) \cdot \mathrm{EESC} + \sum_{j=1}^{N} c_j(t) \cdot X_j(t) + \epsilon(t) \tag{1}$$

$$Y(t) = a(t) + b(t) \cdot t + \sum_{j=1}^{N} c_j(t) \cdot X_j(t) + \epsilon(t) \tag{2}$$

EESC: equivalent effective stratospheric chlorine

t: number of months since start of record (t=1 for January 1979), used in alternative model instead of EESC.

$Y(t)$: target variable, monthly mean total ozone column or ozone partial pressure in month t

$a(t)$: seasonally varying intercept (offset) of the ozone

time series

$b(t)$: seasonally varying EESC or trend coefficient

$X_j(t)$: time series of explanatory variable j (j=1,..,N)

$c_j(t)$: seasonally varying coefficients describing the influence of explanatory variable j

N: Number of explanatory variables in addition to seasonal offset and trend components

$\epsilon(t)$: residual variations not described by the model

Unless we only consider annual mean effects, the regression coefficients $a(t)$, $b(t)$ and $c_j(t)$ are allowed to depend on the month of the year. This time dependence is modelled by 12-month, 6-month, and 4-month sine and cosine harmonic series, i.e.

$$c_j(t) = c_{j,1} + \sum_{k=1}^{3} [c_{j,2k} \cdot \cos(2\pi kt/12) + c_{j,2k+1} \cdot \sin(2\pi kt/12)] \quad (3)$$

and the same formula is used for $a(t)$ and $b(t)$. Thus, usually 7 coefficients need to be estimated for a single proxy time series to account for the fact that the response of ozone to changes in the proxy may vary with season.

The linear regression model was applied to (i) time series of monthly mean total ozone at 30 discrete equivalent latitudes (at 6° resolution) and (ii) to monthly mean stratospheric ozone fields as a function of equivalent latitude (same resolution as total ozone) and pressure. For the latter the CATO fields were interpolated from the native 15 isentropic levels onto 14 discrete pressure levels (190, 120, 90, 60, 40, 30, 20, 15, 10, 7, 5, 3.5, 2.5, 1.5 hPa). Because stratospheric temperatures have a trend on their own, ozone trends on isentropes are not identical to trends on pressure levels. We prefer the representation on pressure levels to be compatible with other trend studies.

Table 1 lists the different explanatory variables together with the source of the data and Fig. 1 shows the individual time series. All proxy data have been developed or

collected as part of the EU project "Chemical and Dynamical Influences on Decadal Ozone Change" (CANDIDOZ). Table 2 additionally shows some characteristic values of the proxies including standard deviations and linear trends for different periods.

In order to represent the influence of the 11-year solar cycle we use the Mg II solar index as suggested by Viereck et al. (2001) since it best describes the variability in solar UV output.

QBO is another proxy that has been traditionally included in ozone trend studies besides solar cycle (World Meteorological Organization, 2003). Because the ozone response shows variable time lags depending on altitude and latitude the QBO is represented here by two separate components, the zonal wind at 10 hPa and at 30 hPa, which are displaced in phase by approximately $\pi/2$. Since any phase lag can be represented by a linear combination of a sine ($\sin(\omega t)$) and a cosine ($\sin(\omega t+\pi/2)$) the model is able to adapt the correct time lag automatically. This method was first proposed by Bojkov et al. (1995) who used a combination of 25 hPa and 50 hPa winds.

The influence of stratospheric aerosols is often represented in statistical models by an updated version of the NASA stratospheric aerosol optical depths data set of Sato et al. (1993). Here we use instead the vertically integrated stratospheric aerosol surface area density (SAD) compiled in the framework of the SPARC Stratospheric Aerosol Assessment (Thomason and Peter, 2006).

As a proxy for the Brewer-Dobson circulation we use the vertical component of the EP flux crossing the 100 hPa pressure surface. In each hemisphere we use the flux spatially averaged over the latitudes 45° to 75° of the respective hemisphere. EP fluxes were calculated from ERA-40 analyses before September 2002 and from operational ECMWF analyses thereafter (Wohltmann et al., 2006[1]).

Polar ozone loss due to reactions on polar stratospheric clouds is represented by the potential volume of PSCs given by the volume of air below the formation temperature of nitric acid trihydrate (NAT) poleward of 60° in the respective hemisphere. Rex et al. (2004) demonstrated that total ozone loss within the polar vortex depends roughly linearly on wintertime accumulated PSC volume. Temperatures were taken from National

Centers for Environmental Prediction (NCEP) reanalyses due to some issues in ERA-40 data (Karpetchko et al., 2005). We have multiplied the PSC volume by EESC to account for the modulation of polar ozone loss by long-term changes in stratospheric chlorine.

In order to account for the cumulating effects of EP flux and PSC volume affecting ozone concentrations several months following their current action, the proxies EPFLUX and VPSC were constructed as

$$X_j(i) = X_j(i-1) \cdot \exp(-\Delta t/\tau) + x_j(i) \quad (4)$$

where $X_j(i)$ is the final EPFLUX or VPSC proxy at time i, Δt is the time step between $i-1$ and i, τ is a suitable 1/e decay time, and $x_j(i)$ is the original (non accumulated) time series of EP flux or PSC volume. Hence, the effects at the same time accumulate and decay with time. In the extratropics the constant τ was set to 12 months during the buildup phase (October to March in the NH and shifted by six months in the SH) and to 3 months during the rest of the year. Fusco and Salby (1999) showed that the wintertime ozone buildup is highly correlated with wintertime accumulated EP flux. Similarly, polar ozone loss is highly correlated with wintertime accumulated PSC volume as mentioned before. Thereafter the ozone columns slowly relax towards a photochemical equilibrium which explains why autumn values are much less variable than springtime columns. Randel et al. (2002) and Fioletov and Shepherd (2003) gave different estimates for this relaxation time scale between 1.5 and "several months". A value of 3 months seems to be a suitable compromise. The results are not very sensitive to this choice (±1 month). We have chosen a much larger value of 12 months for winter to reflect the much longer photochemical lifetime of ozone during these months. In the tropics the photochemical lifetime of ozone is very short and total ozone columns mainly depend on the EP flux of the previous month (Wohltmann et al., 2006[1]). We therefore set τ=1 month between 30° S and 30° N for both proxies.

The proxies VPSC and EPFLUX are negatively correlated with each other (r=−0.45 in the NH for March values). The attribution of variations in ozone to either process

is therefore a delicate problem. When VPSC is excluded from the regression model some of its effects are absorbed by EPFLUX. A more important problem is the high correlation between VPSC and EESC in the Southern Hemisphere (r=0.91 for October values, see Fig. 1) which is due to the fact that the PSC volume does not vary strongly from year to year over Antarctica and due to the way the proxy is constructed. The correlation would be even higher without the exceptional situation in 2002 when the polar vortex split into two parts. Results for the proxy VPSC are therefore only shown for the NH where the correlation with EESC is much smaller (r≈0.38) and a separation between the two effects is still possible.

Autocorrelation in the residual time series $\epsilon(t)$ is accounted for by applying the method of Cochrane and Orcutt (1949). Autocorrelations for lags of up to 3 months were considered. This choice is based on careful inspection of the partial autocorrelations which in many cases showed significant values at lags 1 and 3 and much lower values for larger lags.

3 Results and discussion

If not stated differently the results shown in this section are obtained from a model including all proxies listed in Table 1 with EESC (or alternatively t) describing the anthropogenic influence and covering the period January 1979 to December 2004. In Sect. 3.1 we first discuss the contribution of the proxies to the variability of both total ozone and its vertically resolved stratospheric distribution. Explanatory variables may not only contribute to variability but also to long-term trends. The remaining linear trend in ozone not explained by variables of natural variability (QBO, solar cycle, aerosols and EP flux), which we therefore attribute to the anthropogenic release of ODSs, will be presented in Sect. 3.2. Finally, the recent evolution of ozone since 1996 and its attribution to different factors is analyzed in Sect. 3.3.

3.1 Ozone variability

The influence of the proxies on the variability of total ozone is shown in Fig. 2 as a function of season and equivalent latitude. The contribution of an individual explanatory variable $X_j(t)$ to the variance in total ozone is given by VAR$[c_j(t)X_j(t)]$ plus twice the covariances with other variables (which are usually small). Since the regression coefficients $c_j(t)$ are constant for a given month of the year (see Eq. 3) the variances can also be expressed as $c_j(t)^2 \cdot$VAR$[X_j(t)]$ and standard deviations as $|c_j(t)| \cdot \sigma[X_j(t)]$. In the figure we show values of the signed quantity $c_j(t) \cdot \sigma[X_j(t)]$ which may be interpreted as the percentage change in total ozone resulting from a $1\,\sigma$ increase in the proxy $X_j(t)$. The $1\,\sigma$ values of all proxies are given in Table 2 together with their period mean, minimum and maximum values.

3.1.1 Quasi-biennial oscillation

The QBO signal makes a significant contribution both in a narrow band in the tropics (throughout the year) and in the extratropics poleward of about 15°. A prominent yet insignificant signal is also seen over the North Pole in winter/spring as already noted by Oltmans and London (1982). In the SH roughly the same features are seen as in the NH but displaced by 6 months. Largest amplitudes in the extratropical ozone QBO are observed during winter/spring in the respective hemisphere in agreement with previous findings (e.g. Yang and Tung, 1994; Randel and Wu, 1996) but the signals are significant through most of the year if both components of the QBO at 30 hPa and 10 hPa are considered. The QBO couples to the seasonal cycle in a complex manner as described by Randel and Wu (1996). In a narrow tropical band between 10° N and 10° S total ozone is highest when tropical winds are westerly at 30 hPa (April to July) or somewhere between 10 hPa and 30 hPa (during the rest of the year) in agreement for instance with the study of Yang and Tung (1995). In mid-latitudes, however, the phase lag between total ozone and the QBO is not constant as often assumed in other studies but changes continuously throughout the season. Between July and September, for

instance, total ozone anomalies at northern mid-latitudes are in phase with the QBO at 10 hPa but are in opposite phase between December and March.

The annually averaged contributions of the proxies to the variability of stratospheric ozone as a function of equivalent latitude and pressure are presented in Fig. 3. Annual mean coefficients were obtained using a simplified version of the regression model (Eq. 2) with only one single coefficient estimated per proxy neglecting any seasonal variations. Again, the contributions are shown in terms of percentage change in ozone for a 1 σ increase in the proxy. Note that all signals are damped above about 30–35 km altitude due to the relaxation of CATO to a climatology at these levels (see Sect. 2.1).

The vertical structure of the signals provides additional insight into the total ozone responses. The QBO, for instance, has a profound influence on stratospheric ozone in more or less the whole stratosphere (Figs. 3a and b). However, the response can be at the same time positive and negative at different altitudes. Summing these opposing contributions over a broad altitude range results in destructive interference and bands of mininum response seen in Figs. 2a and b at about 10° and 60°. In the tropics positive QBO anomalies are seen in Fig. 3a simultaneously in the lower (20–27 km) and upper stratosphere (>32 km), and a negative one at 28–32 km. This specific two-cell structure has been explained by Chipperfield et al. (1994) based on model studies by the modulation of the mean vertical transport of O_3 (lower stratosphere) and NO_y (upper stratosphere). Reduced NO_y above 30 km results in less NO_x-catalyzed ozone loss and hence higher O_3. In the tropics there appears to be also a large signal below 100 hPa. However, it should be stressed that these points are located in the upper troposphere where ozone concentrations are comparatively low and the uncertainty of the reconstruction is large (Brunner et al., 2006). Results in the tropical upper troposphere are therefore considered not to be reliable.

The two fields in Figs. 3a and b are similar to the two anomaly patterns SVD1 and SVD2 in Fig. 6 of Randel and Wu (1996) which were obtained by singular value decomposition (SVD) thus representing the two dominating modes of ozone variability associated with the QBO. The similarity with our patterns suggests that the SVD1 and

SVD2 modes basically represent the ozone signatures of the QBO about one quarter cycle ($\pi/2$) out of phase. Using CATO, we are able to extend the patterns beyond the previous limits of 60° S–60° N. We observe distinct signals of the QBO over the poles between about 25 km and 30 km supporting findings of Oltmans and London (1982) and Garcia and Solomon (1987).

3.1.2 Volcanic eruptions

The increased aerosol surface area density following volcanic eruptions affects stratospheric ozone both through changes in heterogeneous chemistry (Solomon et al., 1996) and through changes in dynamics due to the radiative impact of the aerosol (Kodera, 1994). In CATO the effect on total ozone values is most evident at mid to high northern latitudes during the winter and spring months (Fig. 2c). The eruptions of the volcanoes El Chichón (17° N) and Pinatubo (15° N) in 1982 and 1991, respectively, appear to have more strongly perturbed the stratospheric trace gas composition in the NH than in the SH despite the fact that the volcanic aerosol had spread out more or less equally into both hemispheres (Trepte et al., 1993; Jackman et al., 1996). The distribution and timing of the volcanic signal in Fig. 2c agrees well with other observations (e.g. Randel and Wu, 1995). One exception is that the low latitude signature was previously reported to be centered over the equator whereas we find maximum impacts at about 15° on either side of the equator though clearly more pronounced in the SH (see Fig. 2c). The maximum aerosol SAD following Pinatubo was more than five times larger than the standard deviation given in Table 2. This results in maximum ozone depletions of about 2–4% (5–10 DU) at low latitudes, 11–14% (50–60 DU) in Arctic spring and 15–18% (40–50 DU) in Antarctic spring. These numbers agree closely with results from observations (Herman and Larko, 1994; Randel and Wu, 1995) or from numerical simulations (Rosenfield et al., 1997; Jackman et al., 1996) but are higher than in the model study of Kinnison et al. (1994).

In mid-latitudes, the signal is much more significant in the northern hemisphere. It peaks around February and becomes insignificant in August/September. The studies

of Hadjinicolaou et al. (1997, 2002), which are based on 3-D chemistry-transport simulations with parameterized chemistry, suggest that this signal can largely be explained by changes in dynamics following the eruption of Mount Pinatubo. However, the dynamical mechanism remains unclear and 2-D model studies suggest that the radiative impact of the aerosols should rather lead to a slight increase in mid-latitude ozone (Rosenfield et al., 1997).

Over both poles the springtime ozone depletion is enhanced in the presence of volcanic aerosols. The depletion starts in mid-winter at about 60° N and 60° S and then propagates poleward. Over Antarctica the depletion reaches its maximum not before November and hence appears to be significantly delayed relative to the ozone depletion on PSCs expected to peak in October. These results are in good correspondence with the model study of Rosenfield et al. (1997) who explained the delay over the south pole by the effects of the aerosol on photolysis rates leading to more Cl_y being stored as HOCl rather than Cl_2 during polar night. HOCl is less readily photolyzed than Cl_2 leading to a delayed buildup of ClO_x.

The vertical distribution of the annual mean ozone response to volcanic eruptions shows negative values throughout the lower stratosphere maximizing at about 60° where it extends down to the tropopause level in both hemispheres (Fig. 3c). In the SH extratropics the signal mainly occurs below 100 hPa which may explain why it has been missed in previous analyses of satellite data. In the tropics a significantly negative response is found above the tropical tropopause up to about 28 km. In northern mid- to high latitudes there is a change from negative to positive influences at 25 km altitude. This agrees very well with ozone anomalies measured from sondes at Boulder, USA (40° N) (Hofmann et al., 1994), which show a change to positive values at 24 km. The model studies of Rosenfield et al. (1997), Solomon et al. (1996) and Zhao et al. (1997) suggest that in the extratropics the main reason for this change in sign is heterogeneous chemistry on the increased aerosol surface. Heterogeneous reactions reduce the concentration of NO_x but increase ClO_x and HO_x. Reduced NO_x leads to more ozone above 25 km whereas below that level the increases in ClO_x and

HO_x outweigh the reductions in NO_x leading to enhanced ozone depletion. The good agreement of CATO with these studies supports the notion of Solomon et al. (1996) that heterogeneous chemistry played an important role in shaping the ozone response in northern mid-latitudes in addition to the dynamical effects proposed by Hadjinicolaou et al. (1997). Note that the strong signal in the tropical upper troposphere is mostly insignificant.

3.1.3 11-year solar cycle

The effect of the 11-year solar cycle on total ozone is shown in Fig. 2d. An accurate account for solar variability is essential since it may significantly affect ozone trend estimates (World Meteorological Organization, 2003; Steinbrecht et al., 2004). However, until recently such estimates suffered from the temporal alignment of the solar cycles with the eruptions of El Chichón and Pinatubo (Solomon et al., 1996; McCormack et al., 1997; Lee and Smith, 2003). The latest cycle (cycle 23), which peaked between 2000 and 2002, was not synchronized with a major volcanic eruption allowing us to better separate volcanic and solar effects. A further complication is that solar cycle effects at high latitudes are modulated by the QBO (Labitzke and van Loon, 2000), or actually, that the QBO itself might be influenced by the solar cycle (Salby and Callaghan, 2000). Steinbrecht et al. (2003) showed that solar cycle variations in ozone are significantly larger during easterly phases of the QBO (at 50 hPa) than during westerly phases. This kind of splitting of the record according to QBO phase, however, is problematic due to the introduction of aliasing effects (Salby and Callaghan, 2000). Furthermore, the interaction between the annual cycle and the QBO can induce a decadal scale oscillation (Salby et al., 1997). This oscillation happened to be 180° out of phase with the solar flux variation during cycles 21 and 22. Solar variability regression analyses based on this time period are therefore strongly affected by interferences with QBO as demonstrated by Lee and Smith (2003). As for the aerosols, the latest solar cycle was not synchronized with the QBO in the way the previous cycles were and therefore offers the opportunity for better separating the different effects. This may explain some of the

significant differences of our results from these earlier studies.

As shown in Fig. 2d total ozone is generally elevated during periods of maximum solar activity (e.g. Brasseur, 1993; Hood, 1997; Steinbrecht et al., 2003). The low latitude signal appears to be strongest between January and July but seasonal differences are generally small. Similar to the above studies we find that the amplitude of the signal has a local minimum near the equator. The 2-D model study of Brasseur (1993) reported a steady increase in the signal from the equator towards the poles which contrasts with the pattern derived from CATO. Significant regression coefficients are in fact only found between 10° and 35° in the NH and somewhat closer to the equator in the SH. In mid-latitudes the effect is very weak and mostly insignificant. The signal is again larger over the poles during the respective spring seasons in agreement with the study of Brasseur (1993). The modification of polar stratospheric temperatures and geopotential height by the 11-year solar cycle during the northern winter is well documented (Labitzke, 1987; van Loon and Labitzke, 1994) whereas the influence on the high latitude ozone distribution is much less well known due to a lack of observations in this region. Our results indicate that total ozone over Antarctica is sensitive to solar cycle variability both in early winter and late spring. Since the range of Mg II index values is about 3.5 times its standard deviation (Table 2), total ozone is up to 10% higher over Antarctica during solar maximum than during solar minimum which contrast strongly with the value of less than 2% derived by Brasseur (1993). At low latitudes we find the changes to be below 3%.

The vertical pattern of the solar cycle signal is shown in Fig. 3d. For comparison, Fig. 4 shows the same graph for the CATO/SBUV data set in which SBUV profiles were assimilated above 820 K (see Sect. 2.1). This version produces a more realistic picture at altitudes above 30 km where the signal is damped in Fig. 3d due to the relaxation towards an ozone climatology. Note that below 30 km the two figures are very similar and differences are mostly within the uncertainty of the estimated coefficients.

The main feature is a positive response maximizing at about 10–20 hPa (27 to 32 km) with a relatively uniform distribution extending from pole to pole. In the combined

CATO/SBUV data set the signal extends up to about 38 km in mid-latitudes and up to the highest level (>40 km) over Antarctica. The solar cycle signal is generally located at lower altitudes than reported in the model studies of Brasseur (1993), Langematz et al. (2005) and Lee and Smith (2003) (about 32–38 km) but relatively close to the results of Egorova et al. (2005) (30–35 km). It is also substantially lower than reported from previous observation studies. Results based on satellite observations suggested strongest relative increases in ozone from solar minimum to maximum occurring in mid-latitudes near the stratopause between 40 and 50 km (McCormack and Hood, 1996; Wang et al., 1996; Lee and Smith, 2003; Zerefos et al., 2005). Unfortunately, this altitude range is not covered in our analysis. They also found a significant negative signal in the tropical stratosphere at about 30 to 35 km (McCormack and Hood, 1996; Wang et al., 1996; Lee and Smith, 2003) or slightly higher (Zerefos et al., 2005), which is completely absent in our data. We do not find such a signal even if we restrict the analysis to the period 1979–1995 excluding the last solar cycle. A negative signal in the tropical stratosphere contrasts with model results which tend to show a generally positive response maximizing well below 40 km, with either a monopolar structure centered over the tropics (Lee and Smith, 2003), a relatively uniform signal between ±60° (Brasseur, 1993; Egorova et al., 2004, 2005), or showing almost no change in the stratosphere (Huang and Brasseur, 1993). A weak negative signal in the tropical lower stratosphere could only be reproduced by Langematz et al. (2005) which was the first study to include a source of NO_x from high-energy electrons maximizing during solar minimum. The effect of medium-energy electrons during solar maximum or solar proton events, however, was neglected in that study. A similar dipole pattern as in the observations could also be reproduced by Lee and Smith (2003). However, they clearly demonstrated that this is not due to solar cycle variation but rather to the interference with QBO and volcanic eruptions in the statistical analysis.

As in total ozone the largest effects are seen over Antarctica with annually averaged ozone being enhanced by about 7% during solar maximum relative to solar minimum above 30 hPa as well as below 80 hPa. Over the Arctic the signal is generally much

weaker and it is only mildly significant at the upper levels. These observations support the 3-D numerical simulations of Langematz et al. (2005) who found the largest ozone changes at polar latitudes.

3.1.4 Brewer-Dobson circulation

The Brewer-Dobson circulation has a profound impact on total ozone concentrations at high northern latitudes between December and June (Fig. 2e). It explains a dominant fraction of the generally large variability over this region. Between December and February the influence extends down to 40° N. Note that the ozone signal shown in the figure is scaled by the standard deviation of the deseasonalized EP flux time series. It is thus a measure of interannual variability rather than of the seasonal amplitude of variation which would be much larger. An intensified circulation is associated with a weak polar vortex and correspondingly high total ozone values over the poles and reduced values at low latitudes (Fusco and Salby, 1999). Between 30° and 50° N the effect of EP flux variations is minimal. The pattern is similar in the SH but shifted by six months. EP flux is strongest between October and February in the NH and drops to very low values between May and July. The integrated amount of EP flux entering the stratosphere over the winter determines the amount of ozone that is observed in spring. Thereafter ozone concentrations relax towards photochemical equilibrium on a timescale of a few months (Randel et al., 2002; Fioletov and Shepherd, 2003). Total ozone therefore remains correlated to the spring time values and hence to wintertime accumulated EP flux throughout the summer (Fioletov and Shepherd, 2003). This is also seen in Fig. 2e where total ozone anomalies remain significantly influenced by EP flux until the following autumn.

In the SH the situation is somewhat more complicated. The EP flux is generally weaker due to lower wave activity and has a less pronounced annual cycle. Similar to the NH a positive anomaly appears in mid-latitudes in autumn and lasts until the following spring or actually somewhat longer in the SH. Yet, there is a distinct difference between the two hemispheres at polar latitudes. The signal appears much later in the

SH and also the peak influence is delayed by roughly two months. The absence of a strong signal between April and September is likely a consequence of the Antarctic vortex being much more isolated than the Arctic one as already noted by Dobson (1968). The Antarctic vortex is therefore less disturbed by wave activity (and hence variations in EP flux) which may for instance lead to sudden stratospheric warmings in the NH but not in the SH.

The vertical distribution of the annual mean influence of EP flux variations is shown in Fig. 3e. Elevated ozone is mainly found poleward of 60° in the lower stratosphere and down to about 40° above 25 km in both hemispheres. In the SH the positive anomaly in the lower stratosphere extends to lower latitudes which explains the more prominent anomaly seen in the total columns Fig. 2e. The enhanced transport to high latitudes is associated with a decrease in ozone in the tropical lower stratosphere. This is clearly visible up to about 25 km in the NH and somewhat higher up in the SH. Note that in each hemisphere we only accounted for the EP flux of the respective hemisphere. The influence of the NH extratropical pump on the SH and vice versa is excluded in this view.

Figure 5 therefore shows a sequence of the influence of NH EP flux only on the global ozone distribution for selected months. As expected, the influence builds up in the NH from December to March/April and weakens thereafter. The largest buildup occurs north of 60° N below 23 km. Above 25 km a positive anomaly is located at about 50° N in December which slowly progresses northwards until March. The region of reduced ozone in the tropical lower stratosphere (<24 km) extends well into the SH as reported also by Fusco and Salby (1999) based on MLS measurements. Negative ozone responses are not only seen near the equator but at least up to 50° S in the lower stratosphere.

At higher levels above 22–25 km the response to increased EP flux is positive in both hemispheres. Surprisingly, there is a notable positive signal in the SH between December and March at about 50° S. This anomaly may be a consequence of the strongly enhanced upward transport in the SH upper stratosphere (maximum at about

20° S) which produces a strong increase in CH_4 and N_2O from November to February as observed from satellites (Solomon et al., 1986). Using a prognostic model, Solomon et al. (1986) demonstrated that this transport is not induced locally but rather by forcing from the northern hemisphere. Similarly, Salby and Callaghan (2004) analyzed tendencies (e.g. from November to March) of ozone and meteorological parameters and found that amplified wave forcing in the winter hemisphere leads to anomalous upwelling in the summer hemisphere, with largest changes over the polar cap. According to their analysis, the ozone response in the summertime polar stratosphere is thus in phase with the response in the tropics. This is exactly what it seen in Fig. 5 where January and February anomalies are significantly negative in the Antarctic lower stratosphere, in phase with the negative tropical anomalies.

In the NH, the polar anomaly significantly weakens between March and July which is a result of rapid mixing throughout the extratropics once the polar vortex breaks down (Fioletov and Shepherd, 2005). As a result the ozone anomalies remain positive in the lower stratosphere (>100 hPa) in mid-latitudes between May and July. Above 20 km altitude a positive anomaly remains until at least July which is in good agreement with results from a Lagrangian model study by Konopka et al. (2003) which demonstrates that vortex remnants at this level are "frozen in" in the summer circulation without much mixing.

3.1.5 Ozone depletion on PSCs

For reasons described in Sect. 2.2 results for the variable VPSC are only shown for the NH. As expected, the influence on total ozone is strongest between February and April north of 70° N (Fig. 2f). Interestingly, the anomaly spreads to low latitudes, i.e. down to at least 30° N, between April and July suggesting a significant impact of polar ozone depletion on mid-latitude ozone during summer. Notably this effect can not be reproduced by EPFLUX even if VPSC is excluded from the regression model. Given the fact that the range between minimum and maximum PSC volume is four times larger than its standard deviation (see Table 2) we may estimate that mid-latitude ozone is

up to 4% lower in a summer following a cold Arctic winter than following a warm winter due to the effect of polar ozone depletion alone. Using a 3-D chemistry-transport-model, Chipperfield (1999) calculated reductions of 2–3% at 50° N due to the effects of chlorine activation on cold liquid aerosols, NAT and ice particles. Compared to our results these values are too low in particular given the fact that they do not only include polar but also mid-latitude heterogeneous ozone losses. Similar problems have been reported for other numerical simulations (World Meteorological Organization, 2003) but recent model updates have strongly improved the agreement with observed Arctic ozone depletion (Chipperfield et al., 2005). Knudsen and Groß (2000) used reverse domain filling trajectories to calculate the dilution of mid-latitude air by ozone depleted air from the vortex. They found reductions in 30°–60° N mean total ozone due to dilution of the order of 3% in spring 1995 and 1997, respectively, following two exceptionally cold Arctic winters. The dilution effect extends down to about 30° N within the first two months after breakup of the vortex. These results agree well with our estimate of a maximum effect of 4% and the seasonal evolution shown in Fig. 2f.

Unlike the pattern for total ozone the vertical distribution is quite noisy as seen in Fig. 3f. The problems of the regression analysis to distinguish between effects of VPSC and effects of EPFLUX is quite obvious when comparing panels (e) and (f). At high northern latitudes at 17 km for instance, the EP flux signal shows a pronounced minimum. This minimum is compensated by VPSC which shows a distinct negative maximum at the same place. VPSC contributions are largest north of about 65° N as expected, but contributions are also seen in the lower stratosphere (13–17 km) in mid-latitudes. As suggested by Fig. 2f, the latter is probably due to southward transport of polar air depleted in ozone between April and July following the break-up of the polar vortex. The low latitude signals south of 40° N are probably due to the imperfect separation between EP flux and VPSC effects. In a simulation excluding VPSC the EP flux anomalies tend to become more pronounced at these points.

3.2 Ozone trends

Figure 6 compares residual linear trends (coefficient b in Eq. 2) in total ozone estimated for the period 1979 to 1995 (upper panels) and for 1979 to 2004 (lower panels). The term "residual" in this context means that the influence of natural variability, i.e. of volcanic aerosols, solar cycle, EP flux and QBO, on the trend is removed. Results are only shown for the model excluding VPSC because this proxy also contains an anthropogenic component (due to multiplication by EESC) and because of its collinearity with EESC in the SH. The figures can thus be interpreted as representing the overall trend due to man-made increases in EESC which influences both polar processes as well as ozone depletion at non-polar latitudes. The two left-hand panels are linear trends (in %/decade relative to the period mean ozone) whereas the right-hand panels show the influence of EESC (in DU/ppt) directly. Because EESC increased almost linearly between 1979 and 1995 (see Fig. 1) panels (a) and (b) look very similar.

For the period 1979 to 2004, however, the two panels (c) and (d) are distinctly different. The linear trend is significantly smaller than for 1979 to 1995, in particular for mid- to high latitudes in winter and spring in the respective hemisphere. This suggests that even after removing the influences of natural variability the ozone trend was substantially lower (i.e. less negative or even positive) after 1995 than before. The proxy EESC represents the anthropogenic influence more directly. Because EESC reached a maximum in 1997 and started decreasing thereafter it seems to better represent the evolution of ozone than a simple linear trend. The EESC coefficients are in fact similar for both periods (compare panels b and d) confirming that ozone and EESC evolved in a similar way after 1995. This point is analyzed in more detail in Sect. 3.3.

In the NH the largest negative trends are seen in February and March at high equivalent latitudes, i.e. within the polar vortex, with values of up to −13%/decade for 1979–1995 and up to −9%/decade for 1979–2004. Notably there is a second maximum at mid-latitudes around March which seems to be detached from the polar maximum and which occurs too early to be explained by dilution with vortex air. This is likely

an indication of mid-latitude ozone depletion which is thought to be controlled by heterogenous chemistry leading to enhanced chlorine activation (Solomon et al., 1996). Since this process is closely related to the reduction of NO_x by hydrolysis of N_2O_5 on aerosols it is conceivable that its effect is strongest during winter when N_2O_5 hydrolysis is largest. Trends in mid-latitudes are largest in March and are of the order of −5%/decade for 1979–1995 but only −2%/decade for 1979–2004. EESC decreased by 195 ppt from its maximum in 1997 to the end of 2004. Given regression coefficients of about 0.018 DU/ppt in mid-latitudes and 0.055 DU/ppt at polar latitudes this corresponds to an ozone increase since 1997 of up to 3.5 DU in mid-latitudes and up to 11 DU over the Arctic, respectively, due to the effects of the Montreal Protocol. A much larger recovery of the order of 20 DU is expected for Antarctic springtime ozone. However, EESC as used here is not representative for the Arctic and Antarctic stratosphere. Because the air is much older in the polar stratosphere the peak in EESC will likely be delayed here by some 2 to 3 years as compared to mid-latitudes. Hence, a significant increase in ozone owing to the reduction in EESC cannot yet be expected by the end of 2004.

SH mid-latitude trends are similar to those in the NH with values of −3% to −5%/decade for 1979–1995 and about −2% to −3%/decade for 1979–2004. Negative trends tend to be largest in April/May which appears to be too late to be explained by dilution with vortex air depleted in ozone. The seasonal variation of the trend is generally much smaller than in the NH. Near the equator long-term trends are close to zero and mostly insignificant.

Figure 7 shows the vertical distribution of the annual mean linear trend (Fig. 7a) and influence of changes in EESC (Fig. 7b). Largest downward trends (1979–2004) of more than 20%/decade are seen over the Antarctic below 40 hPa (or 25 km), sharply separated at 60° S from the much lower trends of about −5%/decade in mid-latitudes. Significantly negative annual mean downward trends of up to 10%/decade are also seen over the Arctic. The maximum negative trend is located at about 19 km altitude but it is less well confined in latitude as over the Antarctic which reflects the nature of

the Arctic vortex being more perturbed.

The low and mid-latitude trends are remarkably symmetric in the two hemispheres. Both the linear trend and EESC show a vertically well confined band of significant downward trends near 18–20 km altitude extending from about 40° S to 40° N. It peaks at 30° north and south of the equator reaching values of about −8%/decade. A similar layer of large downward trends has also been observed in SAGE-II data but for the shorter period 1984–2000 and with a maximum downward trend of only −4%/decade (World Meteorological Organization, 2003). This feature occurs between the potential temperatures levels 380 K and 470 K in our data set (note that CATO is reconstructed on potential temperature levels). This corresponds to the "tropically controlled region" located between the tropical tropopause and the lower edge of the tropical pipe (Plumb, 1996) in which substantial exchange between tropics and extratropics occurs (Rosenlof et al., 1997). In EESC (panel b) there is no distinct maximum at 30° but rather a smooth transition from high values in the extratropics to lowest values at the equator. This would be consistent with extratropical air depleted in ozone being mixed into the tropics. Above 450 K exchange between tropics and extratropics is strongly reduced (Plumb, 1996) which may explain the limited vertical extent of this feature.

Another region of large negative trends in the upper tropical troposphere is only seen in Fig. 7a. This is not a robust feature as it changes significantly between different versions of both CATO and the regression model and it is not seen in EESC. Ozone partial pressures are low in this region and therefore the large percentage changes concur with only small absolute changes. Note also that trends in the upper stratosphere (around 2 hPa) are underestimated in this version of CATO. Figure 8 therefore shows the trend based on the combined CATO/SBUV data set. In this figure a distinct second maximum in negative trends is seen in the upper stratosphere above the 10 hPa level (above approx. 30 km), in agreement with previous analyzes of SAGE, SBUV and Umkehr data (Randel et al., 1999; Zanis et al., 2006). Note that in terms of relative changes (%/decade) the values would actually increase towards the top of the domain (40 km) reaching values of about 5–6% between 40° and 60° in the southern

and somewhat further poleward in the northern hemisphere. The decrease in trends towards the poles at high altitudes is probably an artefact of the reconstruction method used for this data set. SBUV data were assimilated in geographical coordinates and hence significant parts of the year are not covered by observations at high latitudes, in which case the CATO data set was relaxed towards a climatology.

3.3 Ozone changes since 1996

Recent studies have suggested that first stages of ozone recovery due to the ban of the production of ODSs can already be detected (Newchurch et al., 2003; Reinsel et al., 2005). However, some questions remain whether all natural influence factors such as solar cycle (Steinbrecht et al., 2004) or planetary wave driving (Dhomse et al., 2006) were properly accounted for in these studies. Here we follow a similar approach as Newchurch et al. (2003) to analyze the deviation of ozone from an expected behavior. For this purpose we fitted the regression model to the reference period January 1979 to December 1995 only but analyzed the residuals (measurements minus statistical model prediction) for the full period out to December 2004. As expected, the residuals average close to zero for the reference period over which the model was fitted. If, however, ozone increased faster (slower) than predicted in the following years then the mean R of the residuals for January 1996 to December 2004 will be positive (negative). Using 1996 as reference year is in line with the study of Reinsel et al. (2005) and is motivated by the fact that this roughly corresponds to the time when EESC started to deviate significantly from the linear increase observed before.

Computing R is equivalent to calculating the cumulative sum (CUSUM) of the residuals as done by Newchurch et al. (2003). In their Appendix they provided a formula for the variance VAR(CUSUM) which is composed of three terms representing the variance of the residuals up to 1996, the uncertainty in the mean level of the model fit, and the uncertainty in the trend estimated for the reference period. Because $R = 1/n_2 \cdot \mathrm{CUSUM}$, where n_2 is the number of months between January 1996 and December 2004, the variance of R is given by $\mathrm{VAR}(R) = 1/n_2^2 \cdot \mathrm{VAR(CUSUM)}$. We used this

relation to estimate the 95% confidence level ($|R|>2\sqrt{\mathrm{VAR}(R)}$).

R was calculated for different versions of the model in order to illustrate the effect of adding a specific explanatory variable. Values of R are displayed in Fig. 9 for total ozone as a function of month and equivalent latitude and in Fig. 10 for vertical cross-sections of ozone partial pressures. The different panels show the results for a model including EESC, QBO and solar cycle only (a), adding the effects of volcanic eruptions (b), and adding the effects of EP-flux (c). Panel (d) is for the same model as in (c) except that EESC has been replaced by a linear trend.

When only EESC, QBO and solar flux (SF) are included in the model, values of R are significantly positive in the NH mid- to high latitudes, in particular between winter and early summer (Fig. 9a), suggesting that ozone after 1996 was higher than expected from these classical proxies alone. Adding the effect of volcanic aerosols (b) reduces R substantially in mid-latitudes (and to some extent also in the tropics) leaving only few areas of significantly positive values. The reason for this is that when leaving out the effect of aerosols the model attributes too much of the decrease between 1979 and 1995 to EESC resulting in mostly positive residuals after 1993 when the effect of Pinatubo slowly dissipated. This cannot be fully compensated by the too large increase in model ozone attributed to the increase in EESC after its peak in 1997. Adding EP flux (c) reduces the values of R even further, not only in middle but also at polar latitudes. Hence, changes in wave forcing appear to have contributed to the observed increase in ozone since 1996, in agreement with results presented by Dhomse et al. (2006). However, springtime total ozone is still on average 5 to 10 DU higher than expected between 1996 and 2004 even in the full model, a phenomenon yet unexplained (adding VPSC does not change this).

The situation is somewhat different in the SH. Mid-latitude ozone more or less evolved as expected since 1996. Neither aerosols nor EP flux made a large contribution to the tendency which was dominated by EESC. Significant positive and unexplained deviations are however observed at polar latitudes, especially in autumn (April and May), whereas springtime values have been recovering from decreasing ODSs as

expected.

Figure 9d finally shows the same results as panel (c) when a linear trend is used instead of EESC. Values of R become significantly positive in this case at both middle and high latitudes in both hemispheres suggesting that this model is much less capable of explaining the recent ozone changes. This may be interpreted as a clear sign for the first stage of ozone recovery, i.e. for a significant deviation of the recent trend from the previous negative trend, which is attributable to changes in ODSs. An analysis of the change in trends based on the hockey-stick method (Weatherhead et al., 2000; Reinsel et al., 2005) supports this argument (see Appendix A).

The vertical distribution of ozone partial pressure residuals from 1996 to 2004 is shown in Fig. 10. It is fully consistent with the picture obtained for total ozone. Adding volcanic aerosols has a large effect on the results in the NH lower stratosphere and some effect on the tropical stratosphere. Adding EP-flux further reduces the values of R especially at high northern latitudes. Comparing panels (d) and (c) again demonstrates that large positive residuals remain when we assume a continuation of the negative trend observed between 1979 and 1995, whereas the model using EESC successfully predicts the behavior of ozone after 1996 leaving only few areas of R values significantly different from zero.

4 Conclusions

A multiple linear regression model has been applied to the 26 year long quasi three-dimensional ozone data set CATO to study the influence of the most significant processes on stratospheric ozone including QBO, solar cycle, volcanic eruptions, Brewer-Dobson circulation and polar ozone depletion. The use of equivalent latitude and potential temperature coordinates (ϕ_E, θ) makes the CATO data set insensitive to short-term fluctuations caused by planetary waves which otherwise dominate the variability in total ozone at a given geographical location (Wohltmann et al., 2005). We adopted the process oriented approach presented by Wohltmann et al. (2006)[1] in which the ef-

fects of various climate modes are implicitly but not explicitly included in the regression model. Climate fluctuations associated for instance with NAO may modify the position of troughs and ridges of planetary waves and influence the Brewer-Dobson circulation. These effects are largely accounted for by including EP flux as a proxy for the wave forcing of the stratospheric circulation and by using the (ϕ_E, θ) framework. The extension of ozone satellite records out to 2004 allows for a better separation between the effects of the solar cycle, aerosols and the QBO because the latest solar cycle did not occur synchronously with a major volcanic disturbance and the QBO had a different phase relation than during the previous two cycles.

The QBO was found to have a large influence on ozone variability throughout the stratosphere. Volcanic eruptions (mainly Pinatubo) resulted in negative ozone anomalies in the extratropical lower stratosphere below 25 km and weakly positive anomalies above. In the tropics the region of depleted ozone reaches somewhat higher up. The largest effects in terms of percentage ozone changes were found below 16 km around 60° in both hemispheres. Above that level the effects are much more pronounced in the NH. The solar cycle has a relatively minor positive effect on stratospheric ozone maximizing at about 20° on both sides of the equator as well as over the poles. Our analysis, which is limited to altitudes below 40 km, indicates a maximum effect between 28 and 32 km in the tropics and between about 25 and 38 km in the extratropics, which is lower than suggested by previous studies. Furthermore, we find no negative signal in the tropical lower stratosphere which probably was an artefact of the statistical analysis in previous studies (Lee and Smith, 2003). EP flux has a profound influence on the interannual variability of ozone. Enhanced wave forcing results in large positive anomalies poleward of 60° and negative anomalies in the tropical and subtropical lower stratosphere. Polar stratospheric ozone depletion has only been analyzed for the northern hemisphere, where an up to 4% reduction in mid-latitude total ozone was found following cold Arctic winters, most likely as a result of dilution with air from the vortex.

Long-term trends are much less negative for the period 1979 to 2004 compared to

1979 to 1995 suggesting a levelling off during the recent years. Fitting the model to the period 1979 to 1995 but analyzing the residuals out to 2004 shows that the ozone changes since 1996 can not be understood by assuming a persistent negative trend. A model using EESC instead of a linear trend, on the other hand, quite successfully explains the recent changes, at least when the effects of aerosols and of EP flux changes are accounted for. Even then, lower stratospheric ozone increases since 1996 were somewhat larger in the northern hemisphere during spring and over Antarctica during most of the year than we are presently able to explain.

Appendix A

Hockey-stick analysis of trend since 1996

As suggested by Reinsel et al. (2005) a hockey-stick approach can be used to detect a change in trend after a given reference date relative to the trend before. In this case two separate linear trend components $b_1(t)$ and $b_2(t)$ are included in the regression model which then reads as

$$Y(t) = a(t) + b_1(t) \cdot t + b_2(t) \cdot t_{96} + \sum_{j=1}^{N} c_j(t) \cdot X_j(t) + \epsilon(t) \quad \text{(A1)}$$

where t_{96} is a linear ramp function which is equal to zero before December 1995 and after that is equal to the number of months since December 1995. The coefficient b_1 thus represents the trend between 1979 and 1995, b_2 is the change from this trend, and b_1+b_2 is the absolute trend for the period 1996 to 2004. A positive value of b_2 thus only indicates a positive change but the absolute trend may still be negative if the previous trend b_1 was sufficiently negative. The changes in trend (b_2) and absolute trends (b_1+b_2) for 1996 to 2004 are shown in Fig. 11 for different versions of the model. Large and significant changes in trend (top panels) are seen at middle to high northern latitudes in spring (February–May). Including the effects of aerosols (b) and EP flux

(c) reduces the magnitude of the changes significantly. Absolute trends 1996 to 2004 (bottom panels) are mostly positive in the regions where the largest changes in trends are observed. However, including all explanatory variables (f) reduces the regions of significant absolute trends to the months March to July between 50° and 60° N. Large changes and positive absolute trends are also observed over Antarctica. In southern mid-latitudes the changes in trends are most significant between January and April when quite large negative trends were observed before 1995 (cf. Fig. 6a).

Acknowledgements. We would like to thank MeteoSwiss and the European Center for Medium Range Weather Forecasts (ECMWF) for granting access to the meteorological archive of ERA-40 and operational data. We are very grateful to H.-R. Kuensch for helping develop the methodology used to create CATO. This work has been supported by the European Community grant through the project CANDIDOZ under contract EVK2-CT-2001-00133. CATO is freely available (ASCII tables of monthly means or complete data set of daily fields in netCDF format) through the web page http://www.iac.ethz.ch/cato/ or upon request.

References

Appenzeller, C., Weiss, A. K., and Staehelin, J.: North Atlantic Oscillation modulates total ozone winter trends, Geophys. Res. Lett., 27, 1131–1134, 2000. 6319, 6324

Bodeker, G. E., Scott, J. C., Kreher, K., and McKenzie, R. L.: Global ozone trends in potential vorticity coordinates using TOMS and GOME intercompared against the Dobson network: 1978–1998, J. Geophys. Res., 106, 23 029–23 042, 2001. 6320, 6322

Bodeker, G. E., Shiona, H., and Eskes, H.: Indicators of Antarctic ozone depletion, Atmos. Chem. Phys., 5, 2603–2615, 2005. 6322

Bojkov, R. D., Bishop, L., and Fioletov, V. E.: Total ozone trends from quality-controlled ground-based data (1996–1994), J. Geophys. Res., 100, 25 867–25 876, 1995. 6326

Brasseur, G.: The response of the middle atmosphere to long-term and short-term solar variability: A two-dimensional model, J. Geophys. Res., 98, 23 079–23 090, 1993. 6334, 6335

Brunner, D., Staehelin, J., Künsch, H. R., and Bodeker, G. E.: A Kalman filter reconstruction of the vertical ozone distribution in an equivalent latitude – potential temperature frame-

work from TOMS/GOME/SBUV total ozone observations., J. Geophys. Res., 111, D12308, doi:10.1029/2005JD006279, 2006. 6320, 6321, 6322, 6323, 6330

Chipperfield, M. P.: Multiannual simulations with a three-dimensional chemical transport model, J. Geophys. Res., 104, 1781–1805, 1999. 6339

Chipperfield, M. P., Kinnersley, J. S., and Zawodny, J.: A two-dimensional model study of the QBO signal in SAGE II NO_2 and O_3, Geophys. Res. Lett., 21, 589–592, 1994. 6330

Chipperfield, M. P., Feng, W., and Rex, M.: Arctic ozone loss and climate sensitivity: Updated three-dimensional model study, J. Geophys. Res., 32, L11813, doi:10.1029/2005GL022674, 2005. 6339

Cochrane, D. and Orcutt, G. H.: Application of least squares regression to relationships containing autocorrelated error terms, J. Amer. Stat. Assoc., 44, 32–61, 1949. 6328

Crutzen, P. J.: The influence of nitrogen oxides in the atmospheric ozone content, Quart. J. Roy. Meteorol. Soc., 96, 320–325, 1970. 6319

Dhomse, S., Weber, M., Wohltmann, I., Rex, M., and Burrows, J. P.: On the possible causes of recent increases in northern hemispheric total ozone from a statistical analysis of satellite data from 1979 to 2003, Atmos. Chem. Phys., 6, 1165–1180, 2006. 6320, 6343, 6344

Dobson, G. B. M.: Forty year's research on atmospheric ozone at Oxford: A history, Appl. Opt., 7, 387–405, 1968. 6337

Egorova, T., Rozanov, E., Manzini, E., Haberreiter, M., Schmutz, W., Zubov, V., and Peter, T.: Chemical and dynamical response to the 11-year variability of the solar irradiance simulated with a chemistry-climate model, Geophys. Res. Lett., 31, L06119, doi:10.1029/2003GL019294, 2004. 6335

Egorova, T., Rozanov, E., Zubov, V., Schmutz, W., and Peter, T.: Influence of solar 11-year variability on chemical composition of the stratosphere and mesosphere simulated with a chemistry-climate model, Adv. Space Res., 35, 451–457, 2005. 6335

Farman, J. C., Gardiner, B. G., and Shanklin, J. D.: Large losses of total ozone in Antarctica reveal seasonal ClO_x/NO_x interaction, Nature, 315, doi:10.1038/315207a0, 1985. 6319

Fioletov, V. E. and Shepherd, T. G.: Seasonal persistence of midlatitude total ozone anomalies, Geophys. Res. Lett., 30, 1417, doi:10.1029/2002GL016739, 2003. 6327, 6336

Fioletov, V. E. and Shepherd, T. G.: Summertime total ozone variations over middle and polar latitudes, Geophys. Res. Lett., 32, L04807, doi:10.1029/2004GL022080, 2005. 6338

Fortuin, J. P. F. and Kelder, H.: An ozone climatology based on ozonesonde and satellite measurements, J. Geophys. Res., 103, 31 709–31 734, 1998. 6322

Fusco, A. C. and Salby, M. L.: Interannual variations of total ozone and their relationship to variations of planetary wave activity, J. Climate, 12, 1619–1629, 1999. 6319, 6324, 6327, 6336, 6337

Garcia, R. R. and Solomon, S.: A possible relationship between interannual variability in Antarctic ozone and the quasi-biennial oscillation, Geophys. Res. Lett., 14, 848–851, 1987. 6331

Hadjinicolaou, P., Pyle, J. A., Chipperfield, M. P., and Kettleborough, J. A.: Effect of interannual meteorological variability on mid-latitude O_3, Geophys. Res. Lett., 24, 2993–2996, 1997. 6332, 6333

Hadjinicolaou, P., Jrrar, A., Pyle, J. A., and Bishop, L.: The dynamically driven long-term trend in stratospheric ozone over northern mid-latitudes, Quart. J. Roy. Meteorol. Soc., 128, 1393–1412, 2002. 6319, 6332

Herman, J. R. and Larko, D.: Low ozone amounts during 1992-1993 from Nimbus 7 and Meteor 3 total ozone mapping spectrometers, J. Geophys. Res., 99, 3483–3496, 1994. 6331

Hofmann, D. J., Oltmans, S. J., Komhyr, W. D., Harris, J. M., Lathrop, J. A., Langford, A. O., Deshler, T., Johnson, B. J., Torres, A., and Matthews, W. A.: Ozone loss in the lower stratosphere over the United States in 1992–1993: Evidence for heterogeneous chemistry on the Pinatubo aerosol, Geophys. Res. Lett., 21, 65–68, 1994. 6332

Hood, L. L.: The solar cycle variation of total ozone: Dynamical forcing in the lower stratosphere, J. Geophys. Res., 102, 1355–1370, 1997. 6334

Huang, T. Y. W. and Brasseur, G. P.: Effect of long-term solar variability in a two-dimensional interactive model of the middle atmosphere, J. Geophys. Res., 98, 20 413–20 427, 1993. 6335

Jackman, C. H., Fleming, E. L., Chandra, S., Considine, D. B., and Rosenfield, J. E.: Past, present, and future modeled ozone trends with comparisons to observed trends, J. Geophys. Res., 101, 28 753–28 767, 1996. 6331

Johnston, H.: Reduction of stratospheric ozone by nitrogen oxide catalysts from supersonic transport exhausts, Science, 173, 517–522, 1971. 6319

Karpetchko, A., Kyröö, E., and Knudsen, B. M.: Arctic and Antarctic polar vortices 1957–2002 as seen from the ERA-40 reanalyses, J. Geophys. Res., 110, D21109, doi:10.1029/2005JD006113, 2005. 6327

Kinnison, D. E., Grant, K. E., Connell, P. S., Rotman, D. A., and Wuebbles, D. J.: The chemical and radiative effects of the Mount Pinatubo eruption, J. Geophys. Res., 99, 25 705–25 731, 1994. 6331

Knudsen, B. M. and Groß, J.-U.: Northern mid-latitude stratospheric ozone dilution in spring modeled with simulated mixing, J. Geophys. Res., 105, 6885–6890, 2000. 6339

Koch, G., Wernli, H., Staehelin, J., and Peter, T.: A Lagrangian analysis of stratospheric ozone variability and long-term trens above Payerne (Switzerland) during 1970–2001, J. Geophys. Res., 107, 4373, doi:10.1029/2001JD001550, 2002. 6324

Kodera, K.: Influence of volcanic eruptions on the troposphere through stratospheric dynamical processes in the northern hemisphere winter, J. Geophys. Res., 99, 1273–1282, 1994. 6331

Konopka, P., Groß, J.-U., Bausch, S., Müeller, R., McKenna, D. S., Morgenstern, O., and Orsolini, Y.: Dynamics and chemistry of vortex remnants in late Arctic spring 1997 and 2000: Simulations with the Chemical Lagrangian Model of the Stratosphere (CLaMS), Atmos. Chem. Phys., 3, 839–849, 2003. 6338

Labitzke, K.: Sunspots, the QBO, and the stratospheric temperature in the north polar region, Geophys. Res. Lett., 14, 535–537, 1987. 6334

Labitzke, K. and van Loon, H.: The QBO effect on the solar signal in the global stratosphere in the winter of the Northern Hemisphere, J. Atmos. Sol-Terr. Phys., 62, 621–628, 2000. 6333

Langematz, U., Grenfell, J. L., Matthes, K., Mieth, P., Kunze, M., Steil, B., and Brühl, C.: Chemical effects in 11-year solar cycle simulations with the Freie Universität Berlin Climate Middle Atmosphere Model with online chemistry (FUB-CMAM-CHEM), Geophys. Res. Lett., 32, L13803, doi:10.1029/2005GL022686, 2005. 6335, 6336

Lee, H. and Smith, K.: Simulation of the combined effects of solar cycle, quasi-biennial oszillation, and volcanic forcing on stratospheric ozone changes in recent decades, J. Geophys. Res., 108, 4049, doi:10.1029/2001JD001503, 2003. 6333, 6335, 6346

McCormack, J. P. and Hood, L. L.: Apparent solar cycle variations of upper stratospheric ozone and temperature: Latitude and seasonal dependencies, J. Geophys. Res., 101, 20 933–20 944, 1996. 6335

McCormack, J. P., Hood, L. L., Nagatani, R., Miller, A. J., Planet, W. G., and McPeters, R. D.: Approximate separation of volcanic and 11-year signals in the SBUV-SBUV/2 total ozone record over the 1979–1995 period, Geophys. Res. Lett., 24, 2729–2732, 1997. 6333

Molina, M. J. and Rowland, F. S.: Stratospheric sink for chlorofluoromethanes: Chlorine atom-catalysed destruction of ozone, Nature, 249, 810–812, 1974. 6319

Newchurch, M. J., Yang, E.-S., Cunnold, D. M., Reinsel, G. C., Zawodny, J. M., and Russell III, J. M.: Evidence for slowdown in stratospheric ozone loss: First stage of ozone recovery., J. Geophys. Res., 108, 4507, doi:10.1029/2003JD003471, 2003. 6319, 6343

Oltmans, S. J. and London, J.: The quasi-biennial oscillation in atmospheric ozone, J. Geophys. Res., 87, 8981–8989, 1982. 6329, 6331

Plumb, R. A.: A "tropical pipe" model of stratospheric transport, J. Geophys. Res., 101, 3957–3972, 1996. 6342

Randel, W. J. and Wu, F.: TOMS total ozone trends in potential vorticity coordinates, Geophys. Res. Lett., 22, 683–686, 1995. 6331

Randel, W. J. and Wu, F.: Isolation of the ozone QBO in SAGE II data by singular-value decomposition, J. Atmos. Sci., 53, 2546–2559, 1996. 6329, 6330

Randel, W. J. and Wu, F.: A stratospheric ozone trends data set for global modeling studies, Geophys. Res. Lett., 26, 3089–3092, 1999. 6321

Randel, W. J., Stolarski, R. S., Cunnold, D. M., Logan, J. A., and Newchurch, M. J.: Trends in the vertical distribution of ozone, Science, 285, 1689–1692, 1999. 6342

Randel, W. J., Wu, F., and Stolarski, R.: Changes in column ozone correlated with the stratospheric EP flux, J. Meteorol. Soc. Japan, 80, 849–862, 2002. 6327, 6336

Reinsel, G. C., Weatherhead, E. C., Tiao, G. C., Miller, A. J., Nagatani, R. M., Wuebbles, D. J., and Flynn, L. E.: On detection of turnaround and recovery in trend for ozone, J. Geophys. Res., 107, 4078, doi:10.1029/2001JD000500, 2002. 6319

Reinsel, G. C., Miller, A. J., Weatherhead, E. C., Flynn, L. E., Nagatani, R. M., Tiao, G. C., and Wuebbles, D. J.: Trend analysis of total ozone data for turnaround and dynamical contributions, J. Geophys. Res., 110, D16306, doi:10.1029/2004JD004662, 2005. 6319, 6343, 6345, 6347

Rex, M., Salawitch, R. J., von der Gathen, P., Harris, N. R. P., Chipperfield, M. P., and Naujokat, B.: Arctic ozone loss and climate change, Geophys. Res. Lett., 32, L04116, doi:10.1029/2003GL018844, 2004. 6324, 6326

Rind, D., Perlwitz, J., and Lonergan, P.: AO/NAO response to climate change: 1. Respective influences of stratospheric and tropospheric climate changes, J. Geophys. Res., 110, D12107, doi:10.1029/2004JD005103, 2005. 6324

Rosenfield, J. E., Considine, D. B., Meade, P. E., Bacmeister, J. T., Jackman, C. H., and Schoeberl, M. R.: Stratospheric effects of Mount Pinatubo aerosol studied with a coupled two-dimensional model, J. Geophys. Res., 102, 2649–3670, 1997. 6331, 6332

Rosenlof, K. H., Tuck, A. F., Kelly, K. K., Russel, J. M., and McCormick, M. P.: Hemispheric asymmetries in water vapor and inferences about transport in the lower stratosphere, J. Geophys. Res., 102, 13 213–13 234, 1997. 6342

Salby, M. and Callaghan, P.: Connection between the solar cycle and the QBO: The missing link, J. Climate, 13, 2652–2662, 2000. 6333
Salby, M., Callaghan, P., and Shea, D.: On the interdependence of the tropical and extratropical QBO and its relationship to the solar cycle, J. Geophys. Res., 102, 29 789–29 798, 1997. 6320, 6333
Salby, M. L. and Callaghan, P. F.: Interannual changes of the stratospheric circulation: Influence on the tropics and southern hemisphere, J. Climate, 17, 952–964, 2004. 6338
Sato, M., Hansen, J., McCormack, M., and Pollack, J.: Stratospheric aerosol optical depth, J. Geophys. Res., 98, 1850–1890, 1993. 6326
Schnadt, C. and Dameris, M.: Relationship between North Atlantic Oscillation changes and stratospheric ozone recovery in the Northern Hemisphere in a chemistry-climate model, J. Geophys. Res., 30, 1487, doi:10.1029/2003GL017006, 2003. 6324
Schoeberl, M. R., Lait, L. R., Newman, P. A., Martin, R. L., Proffitt, M. H., Hartmann, D. L., Loewenstein, M., Podolske, J., Strahan, S. E., and Gary, B.: Reconstruction of the constituent distribution and trends in the Antarctic polar vortex from ER-2 flight observations, J. Geophys. Res., 94, 16 815–16 845, 1989. 6320
Solomon, S., Kiehl, J. T., Garcia, R. R., et al.: Tracer transport by the diabatic circulation deduced from satellite observations, J. Atmos. Sci., 43, 1603–1617, 1986. 6338
Solomon, S., Portmann, R. W., Garcia, R. R., Thomason, L. W., Poole, L. R., and McCormick, M. P.: The role of aerosol variations in anthropogenic ozone depletion at northern mid-latitudes, J. Geophys. Res., 101, 6713–6728, 1996. 6320, 6331, 6332, 6333, 6341
Staehelin, J., Harris, N. R. P., Appenzeller, C., Eberhard, J., and Piechowski, M.: Observations of ozone trends, Rev. Geophys., 39, 231–290, 2001. 6319
Steinbrecht, W., Claude, H., Köhler, U., and Hoinka, K. P.: Correlation between tropopause height and total ozone: Implication for long-term trends, J. Geophys. Res., 103, 19 183–19 192, 1998. 6319
Steinbrecht, W., Hassler, B., Claude, H., Winkler, P., and Stolarski, R. S.: Global distribution of total ozone and lower stratospheric temperature variations, Atmos. Chem. Phys., 3, 1421–1438, 2003. 6333, 6334
Steinbrecht, W., Claude, H., and Winkler, P.: Enhanced upper stratospheric ozone: Sign of recovery or solar cycle effect?, J. Geophys. Res., 109, D02308, doi:10.1029/2003JD004284, 2004. 6320, 6333, 6343
Stolarski, R. S. and Cicerone, R. J.: Stratospheric chlorine: A possible sink for ozone, Can. J.

Chem., 52, 1610–1615, 1974. 6319
Stolarski, R. S., Bloomfield, P., McPeters, R. D., and Herman, J. R.: Total ozone trends deduced from Nimbus 7 TOMS data, Geophys. Res. Lett., 18, 1015–1018, 1991. 6319, 6324
Thomason, L. W. and Peter, T.: The Assessment of stratospheric aerosol properties, SPARC Newsletter 26, SPARC, Toronto, ON, Canada, 2006. 6326
Trepte, C. R., Viega, R. E., and McCormick, M. P.: The poleward dispersal of the Mount Pinatubo volcanic aerosol, J. Geophys. Res., 98, 18 563–18 573, 1993. 6331
van Loon, H. and Labitzke, K.: The 10-12 year atmospheric oscillation, Meteorol. Z., 3, 259–266, 1994. 6334
Viereck, R. A., Puga, L. C., Judge, D., Weber, M., and Tobiska, W. K.: The Mg II index: A proxy for solar EUV, Geophys. Res. Lett., 28, 1343–1346, 2001. 6326
Wang, H. J., Cunnold, D. M., and Bao, X.: A critical assessment of Stratospheric Aerosol Gas Experiment ozone trends, J. Geophys. Res., 101, 12 495–12 514, 1996. 6335
Wang, H. J., Cunnold, D. M., Thomason, L. W. T., Zawodny, J. M., Joseph, M., and Bodeker, G. E.: Assessment of SAGE V6.1 ozone data quality, J. Geophys. Res., 107, 4691, doi:10.1029/2002JD002418, 2002. 6321
Weatherhead, E. C. and Andersen, S. B.: The search for signs of recovery of the ozone layer, Nature, 441, 39–45, doi:10.1038/nature04746, 2006. 6319
Weatherhead, E. C., Reinsel, G. C., Tiao, G. C., Jackman, C. H., Bishop, L., Frith, S. M. H., DeLuisi, J., Keller, T., Oltmans, S., Fleming, E., Wuebbles, D., Kerr, J., Miller, A., Herman, J., McPeters, R., Nagatani, R., and Frederick, J.: Detecting the recovery of total column ozone, J. Geophys. Res., 105, 22 201–22 210, 2000. 6319, 6345
Weiss, A. K., Staehelin, J., Appenzeller, C., and Harris, N. R. P.: Chemical and dynamical contributions to ozone profile trends of the Payerne (Switzerland) balloon soundings, J. Geophys. Res., 106, 22 685–22 694, 2001. 6324
Wohltmann, I., Rex, M., Brunner, D., and Mäder, J.: Integrated equivalent latitude as a proxy for dynamical changes in ozone column, Geophys. Res. Lett., 32, L09811, doi:10.1029/2005GL022497, 2005. 6323, 6324, 6345
World Meteorological Organization: Scientific assessment of ozone depletion: 1994, Global Ozone Research and Monitoring Project, Geneva, Switzerland, report No. 37, 1995. 6319
World Meteorological Organization: Scientific assessment of ozone depletion: 2002, Global Ozone Research and Monitoring Project, Geneva, Switzerland, report No. 47, 2003. 6319, 6326, 6333, 6339, 6342

Yang, H. and Tung, K. K.: Statistical significance and pattern of extratropical QBO in column ozone, Geophys. Res. Lett., 21, 2235–2238, 1994. 6329

Yang, H. and Tung, K. K.: On the phase propagation of extratropical ozone quasi-biennial oscillation in observational data, J. Geophys. Res., 100, 9091–9100, 1995. 6329

Zanis, P., Maillard, E., Staehelin, J., Zerefos, C., Kosmidis, E., Tourpali, K., and Wohltmann, I.: On the turnaround of stratospheric ozone trends deduced from the re-evaluated Umkehr record of Arosa, Switzerland, J. Geophys. Res., in press, 2006. 6342

Zerefos, C. S., Tourpali, K., and Balis, D.: Solar activity-ozone relationships in the vertical distribution of ozone, Int. J. Remote Sens., 26, 3449–3454, 2005. 6335

Zhao, X., Turco, R. P., Kao, C.-Y. J., and Elliot, S.: Aerosol-induced chemical perturbations of stratospheric ozone: Three-dimensional simulations and analysis of mechanisms, J. Geophys. Res., 102, 3617–3637, 1997. 6332

Ziemke, J. R., Chandra, S., McPeters, R. D., and Newman, P. A.: Dynamical proxies of column ozone with application to global trend models, J. Geophys. Res., 102, 6117–6129, 1997. 6324

Table 1. List of explanatory variables used in the regression model. Copies of these proxy data sets can be obtained from http://fmiarc.fmi.fi/candidoz/proxies.html.

Proxy	Description	Source
SOLAR	Mg II index (core to wing ratio)	http://www.iup.physik.uni-bremen.de/gome/gomemgii.html
QBO10	QBO at 10 hPa measured at Singapore	Courtesy of B. Naujokat (FU Berlin)
QBO30	QBO at 30 hPa measured at Singapore	Courtesy of B. Naujokat (FU Berlin)
AERO	Volcanic aerosols, vertically integrated aerosol surface area per unit surface	SPARC Stratospheric Aerosol Assessment http://www-sparc.larc.nasa.gov/
EPFLUX	Vertical component of EP flux at 100 hPa averaged over 45°–75° north and south	NCEP data processed by AWI Potsdam, http://www.awi-potsdam.de/www-pot/atmo/candidoz/
EESC	Equivalent effective stratospheric chlorine	Europ. Environ. Agency, http://dataservice.eea.eu.int/dataservice/viewdata/viewtbl.asp?id=52&i=1&res=3
VPSC	PSC volume in northern hemisphere multiplied by EESC	NCEP data processed by AWI Potsdam, http://www.awi-potsdam.de/www-pot/atmo/candidoz/

Table 2. Statistics of the monthly values of the explanatory variables for the period 1979–2004, and linear trend fits for three selected periods. For some proxies two separate time series were used for the northern (-N) and southern (-S) hemisphere.

Proxy	Units	Mean	1σ	Min	Max	Trend/dec 1979–1995	Sig [1]	Trend/dec 1979–2004	Sig	Trend/dec 1996–2004	Sig
SOLAR	none	1383	512	687	2472	−352	***	−108	**	728	***
QBO10	0.1 m/s	−7.57	19.26	−38.3	24.6	−1.16		1.71		4.55	
QBO30	0.1 m/s	−7.21	18.11	−35.5	17.8	2.21		0.70		10.13	
AERO-N	$10^4 \mu m^2\, cm^{-2}$	216	328	0	1712	248	***	−56	*	−18	***
AERO-S	$10^4 \mu m^2\, cm^{-2}$	253	370	0	2015	339	***	−46	.	−48	***
EESC	ppt	2839	476	1847	3352	888	***	585	***	−247	***
EPFLUX-N [2]	$10^5\, kg\, s^{-2}$	0.00	0.25	−0.93	0.83	0.08	*	0.11	***	0.37	***
EPFLUX-S [2]	$10^5\, kg\, s^{-2}$	0.00	0.16	−0.45	0.46	0.23	***	0.13	***	−0.07	.
VPSC-N [2]	$10^{18}\, m^3$ ppt	0	91	−160	511	45	***	29	***	−155	***
VPSC-S [2]	$10^{18}\, m^3$ ppt	0	428	−127	1290	546	***	416	***	−389	***

[1] Significance of trend (p-values): 0 "***" 0.001 "**" 0.01 "*" 0.05 "." 0.1. Thus one or more stars indicates value is significant at 95% level.

[2] All values are given for the deseasonalized data because proxy exhibits strong seasonal cycle.

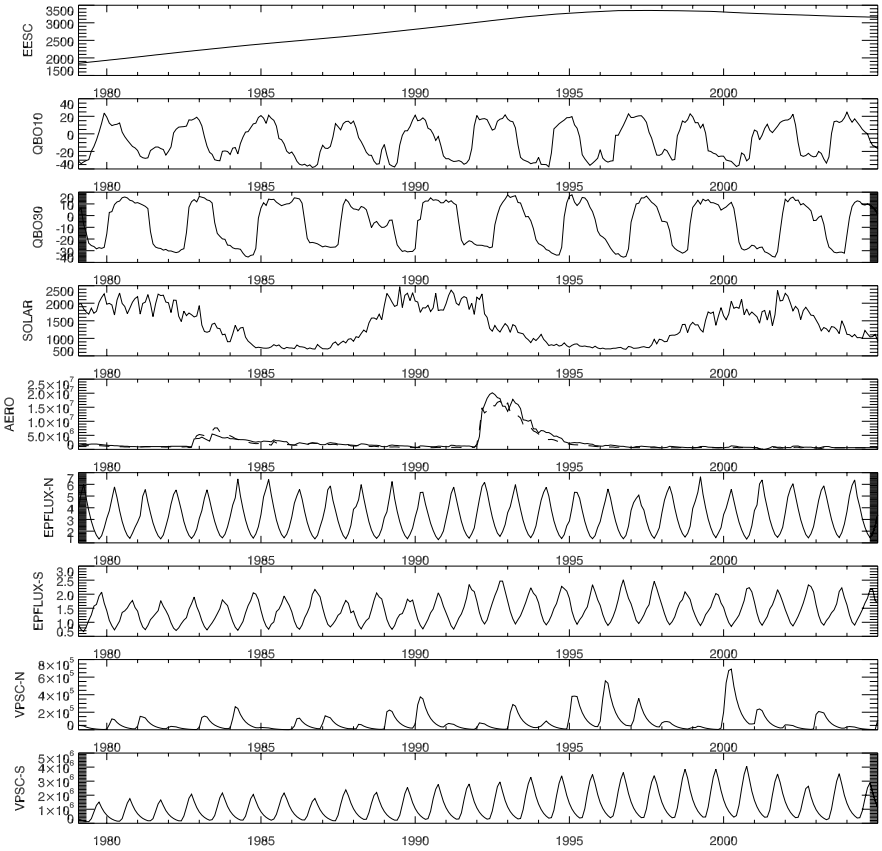

Fig. 1. The time series of monthly proxy data (see also Table 2) from January 1979 to December 2004. The dashed line in panel AERO is the northern hemisphere mean, the solid line the southern hemisphere mean. Tick marks indicate January of each year.

ACPD
6, 6317–6368, 2006

EGU

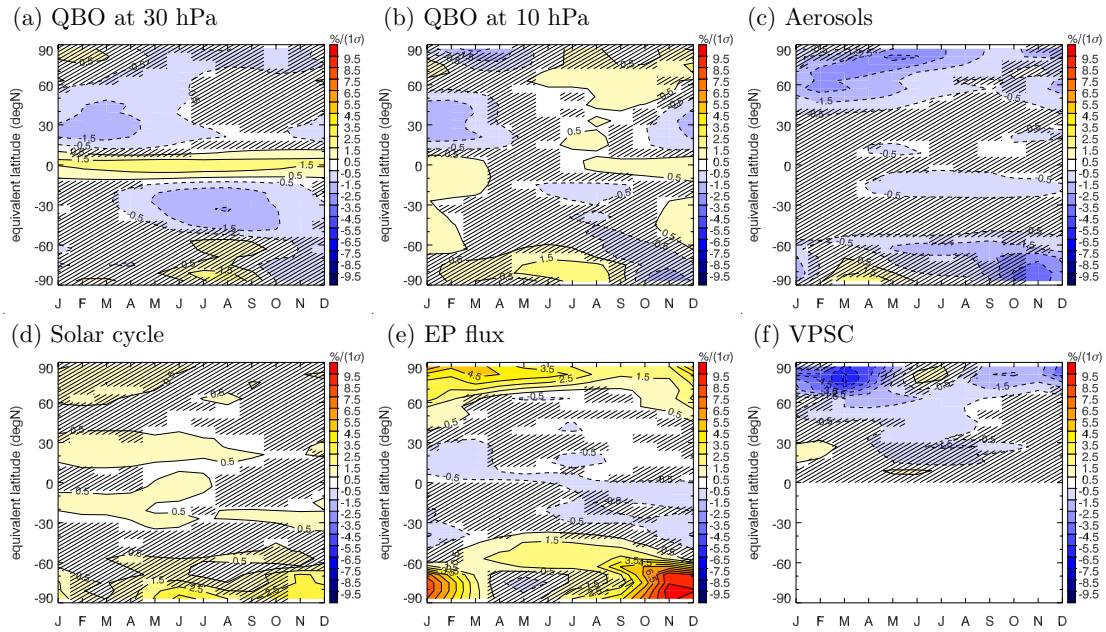

Fig. 2. Contributions to variability in total ozone as a function of season and equivalent latitude. To show all figures in comparable units the regression coefficients were first multiplied by one standard deviation of each proxy time series and then divided by the 1979–2004 mean ozone distribution. Values thus represent the percent change in total ozone for a 1 σ increase in the corresponding proxy. Shading indicates that the values are statistically not significant at the 95% significance level. Contour line spacing is 1%.

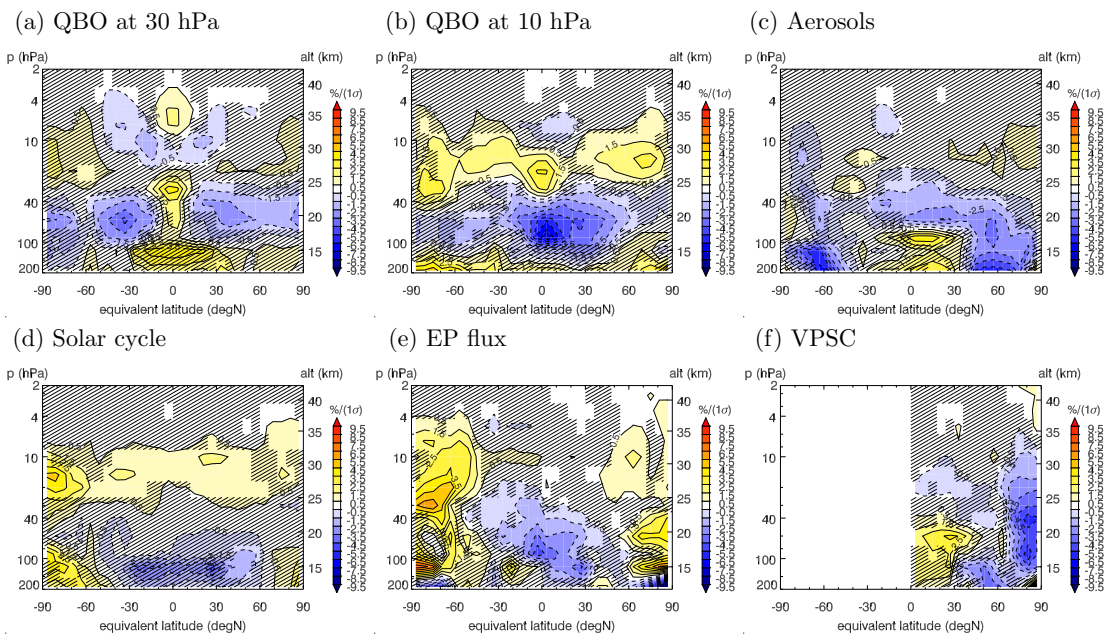

Fig. 3. Annual average contributions to variability in ozone partial pressure as a function of equivalent latitude and pressure. Values are given as percent change in ozone for a 1 σ change in the corresponding proxy. See Fig. 2 for further details.

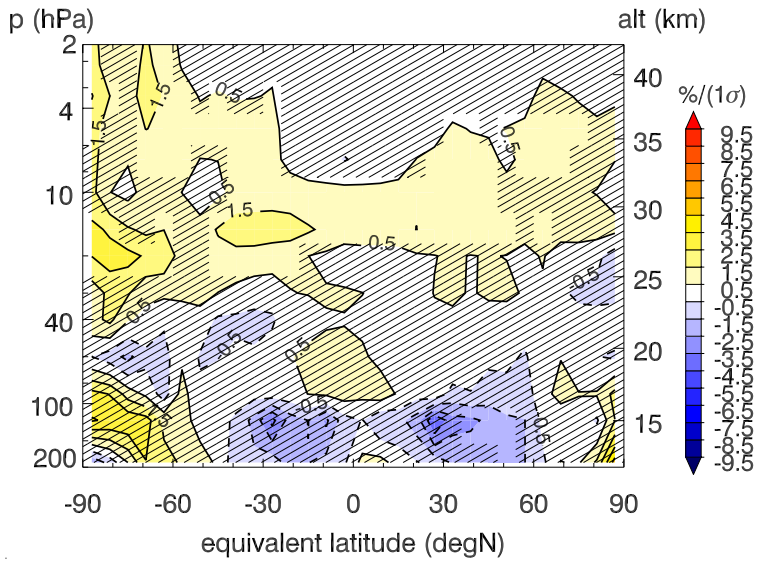

Fig. 4. 11-year solar cycle signal in CATO version with SBUV Version 8 data assimilated in upper stratosphere.

ACPD
6, 6317–6368, 2006

EGU

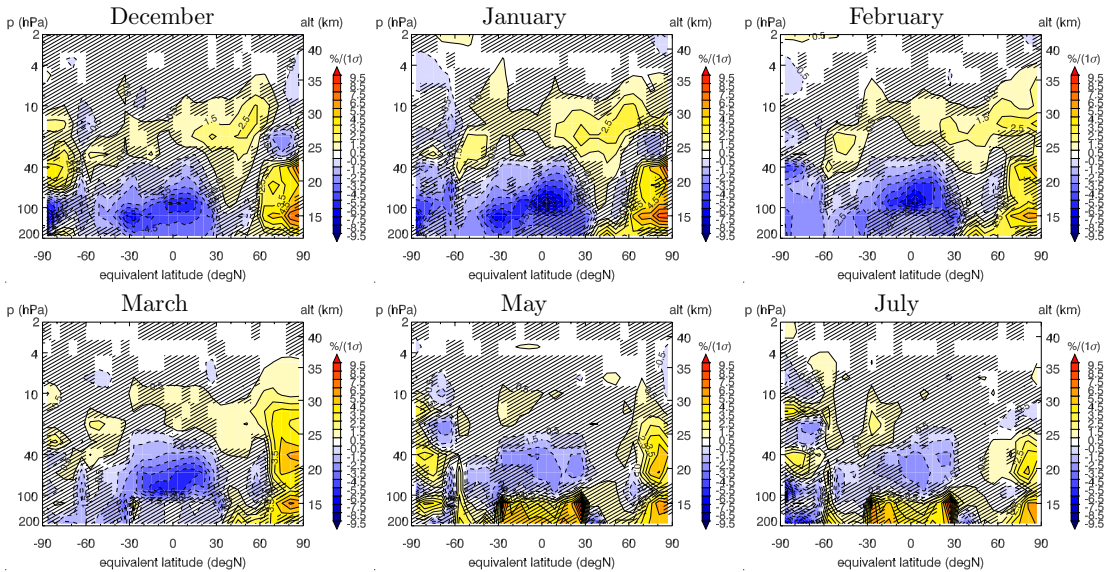

Fig. 5. Sequence of the influence of northern hemisphere EP flux variations on the global stratospheric ozone distribution in selected months.

ACPD
6, 6317–6368, 2006

EGU

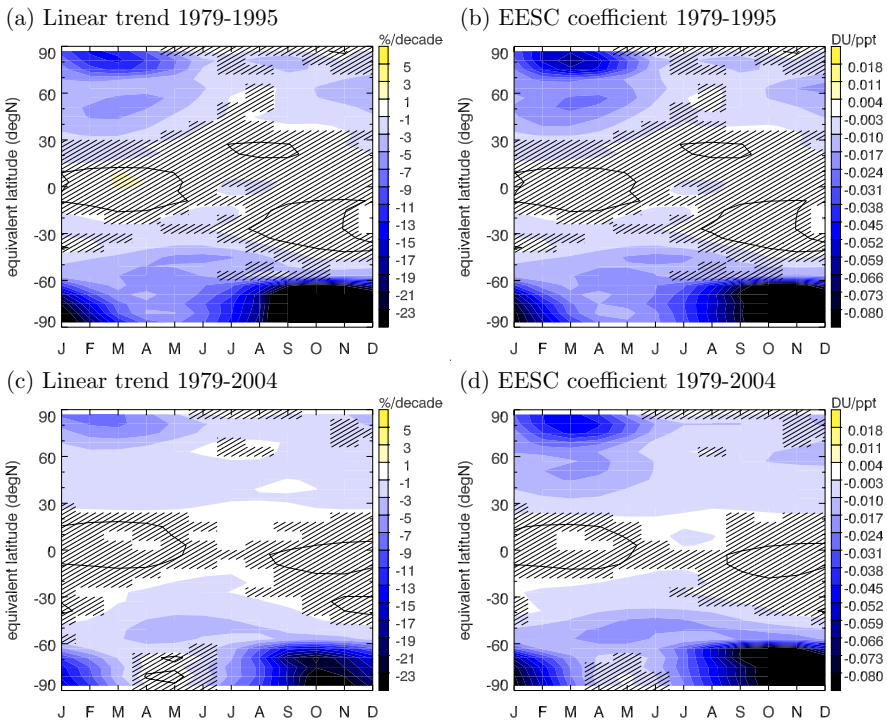

Fig. 6. Model estimates of the anthropogenic influence on ozone trends. Panels **(a)** and **(c)** show the linear trend component (coefficient *b*) in percent per decade for two different time periods, 1979–1995 and 1979–2004, respectively, for the full model but excluding the influence of VPSC. Panels **(b)** and **(d)** show the influence of changes in EESC on total ozone (DU/ppt) calculated with the same model but with EESC instead of a simple linear trend.

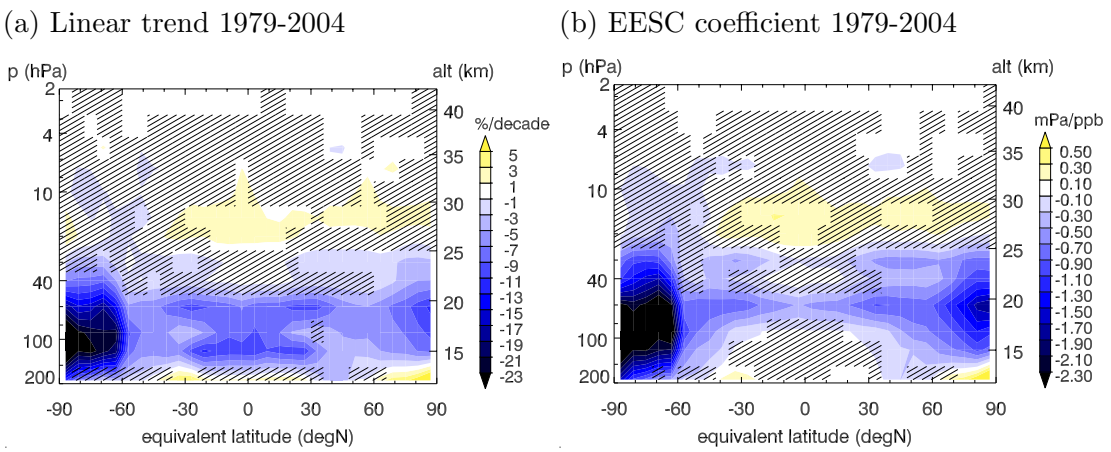

Fig. 7. Model estimates of the anthropogenic influence on ozone profile trends. **(a)** Linear trend component (coefficient *b*) in percent per decade for the full model but excluding the influence of VPSC. **(b)** Influence of changes in EESC on ozone partial pressure (mPa/ppb) calculated with the same model as (a) but with EESC instead of a linear trend.

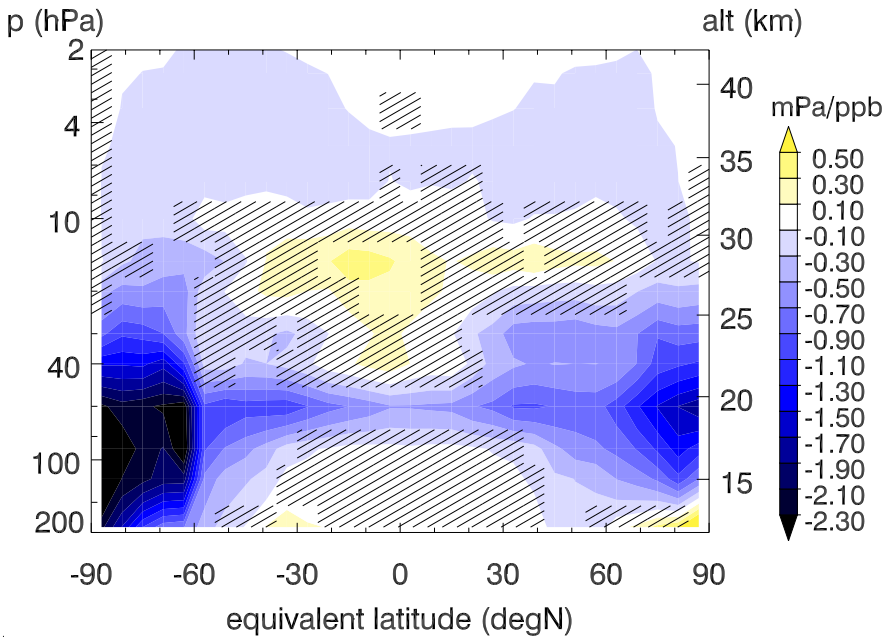

Fig. 8. Same as Fig. 7b but for CATO version with SBUV Version 8 data assimilated in upper stratosphere and only for the period 1979–2003.

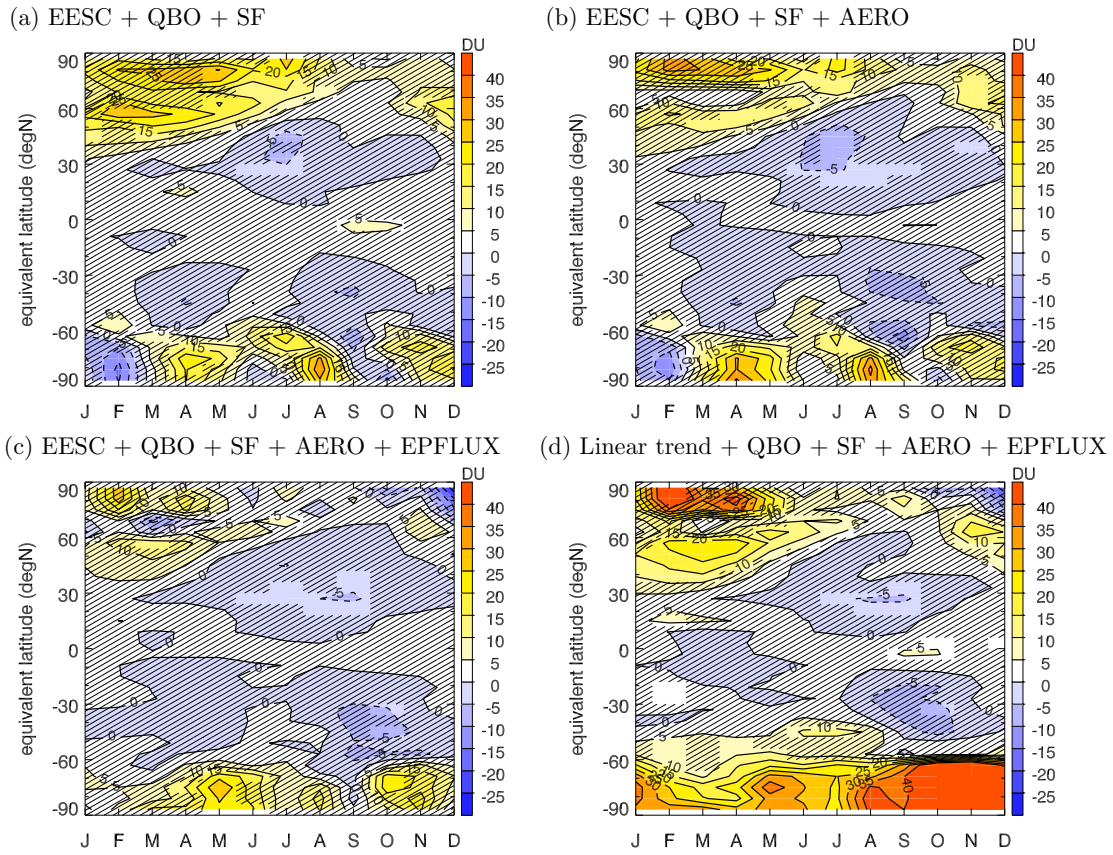

Fig. 9. Mean of total ozone residuals 1996–2004 for different model versions fitted to period January 1979 to December 1995. **(a)** Model including the effects of EESC, QBO and solar cycle only. **(b)** Same as (a) but including the effect of volcanic eruptions. **(c)** Same as (b) but including effect of Eliassen-Palm flux. **(d)** Same as (c) but fitting a linear trend instead of EESC.

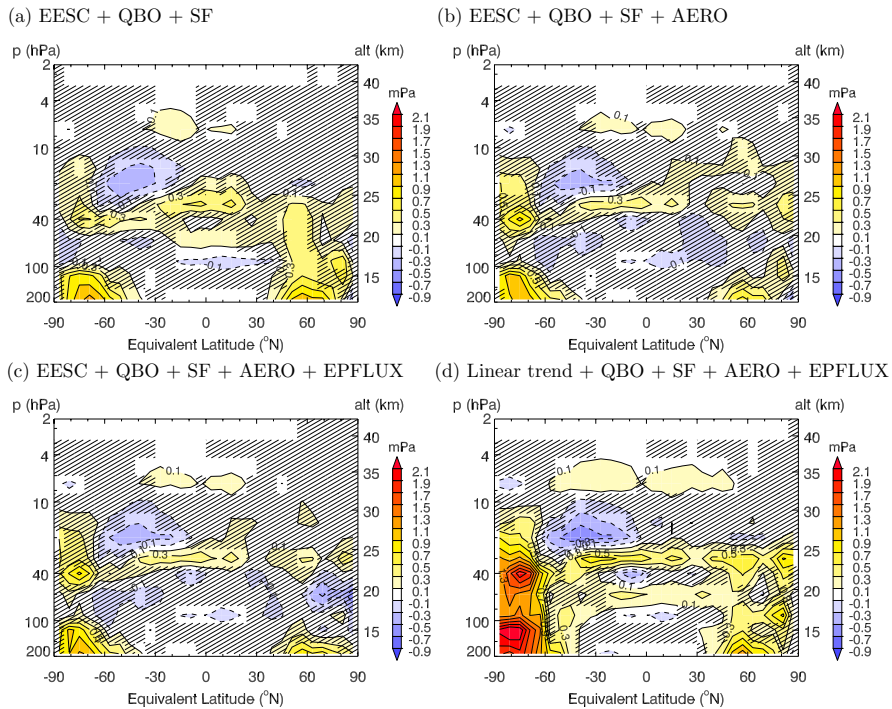

Fig. 10. Vertical cross-section of the mean ozone partial pressure residuals 1996–2004 for different model versions fitted to period January 1979 to December 1995. **(a)** Model including the effects of EESC, QBO and solar cycle only. **(b)** Same as (a) but including the effect of volcanic eruptions. **(c)** Same as (b) but including effect of Eliassen-Palm flux. **(d)** Same as (c) but fitting a linear trend instead of EESC.

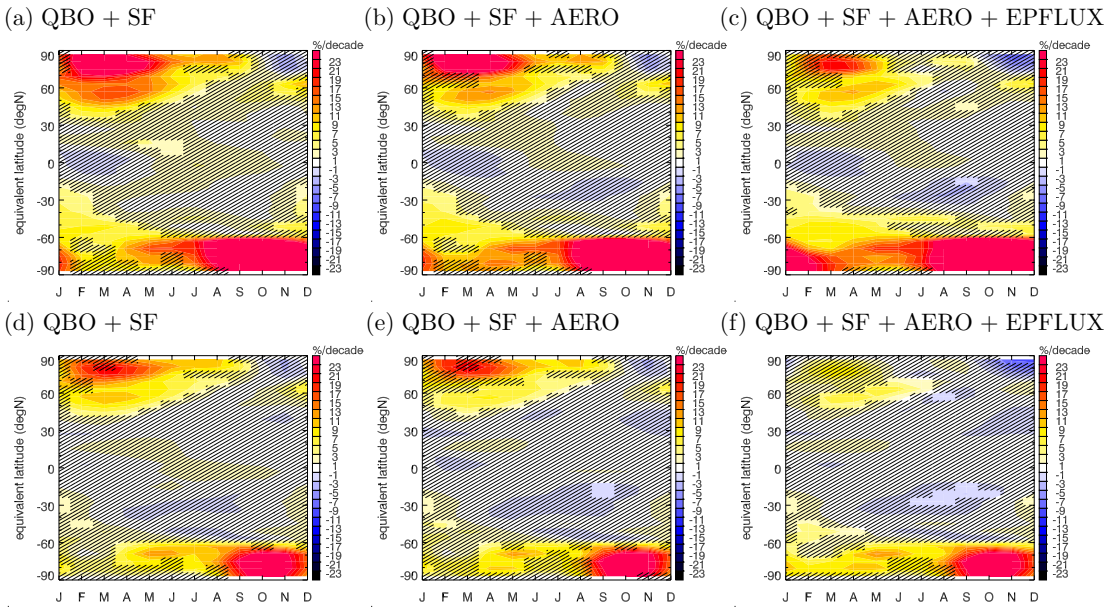

Fig. 11. Results of hockey-stick analysis with two different trends before and after December 1995. Top row: Change in trend (coeff. b_1) for period 1996–2004 as compared to period 1979–1995. Bottom row: Absolute trend (b_1+b_2) for period 1996–2004.